Multiplexed Holographic Data Storage in

Bacteriorhodopsin

Final Performance Report [NASA Grant - NAG 2-1077]

Submitted to the

NASA Ames Research Center
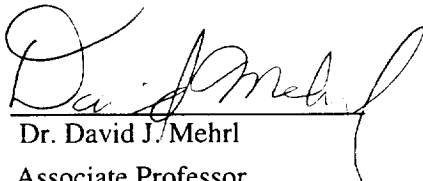
MS 241-1

Moffett Field, CA 94035

by the

Optical Systems Laboratory

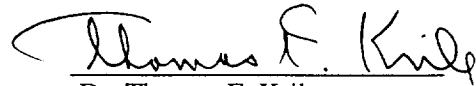Department of Electrical Engineering

Texas Tech University

Lubbock, TX 79409-3102

June, 1999

Dr. David J. Mehrl
Associate Professor
Principal Investigator

Dr. Thomas F. Krile
Professor
Co-Principal Investigator

MULTIPLEXED HOLOGRAPHIC DATA STORAGE IN BACTERIORHODOPSIN

Summary of Technical Accomplishments

Biochrome photosensitive films in particular Bacteriorhodopsin exhibit features which make these materials an attractive recording medium for optical data storage and processing. Bacteriorhodopsin films find numerous applications in a wide range of optical data processing applications; however the short-term memory characteristics of BR limits their applications for holographic data storage. The life-time of the BR can be extended using cryogenic temperatures [1], although this method makes the system overly complicated and unstable. Longer life-times can be provided in one modification of BR - the "blue" membrane BR [2], however currently available films are characterized by both low diffraction efficiency and difficulties in providing photoreversible recording. In addition, as a dynamic recording material, the BR requires different wavelengths for recording and reconstructing of optical data in order to prevent the information erasure during its readout. This fact also put constraints on a BR-based Optical Memory, due to information loss in holographic memory systems employing the two-lambda technique for reading-writing thick multiplexed holograms [3].

Thus, we concentrated our efforts on the solution of the following problems:

1. Investigate volume holograms recording and reconstruction in 2-λ geometry in the general case when reference and readout waves are highly divergent spherical beams.
2. Experimentally performed multiplexed holograms recording using available short life-time BR films in order to verify our theoretical model.
3. Developed the means to circumvent the limitation on the optical storage density peculiar to the Holographic Memory systems exploiting the 2-λ technique.
4. Investigated hologram recording regimes using long life-time states of the BR.
5. Investigated features of the BR for achieving nonvolatile readout of the stored information.
6. Investigated applications of the BR in the system supporting Optical Memory modules (SLM, optical interconnection, etc.)

We devised a simplified analysis/calculation scheme for calculating critical parameters of the holographic memory system employing highly divergent reference/readout beams and different wavelengths for data recording and reconstruction [1,2]. Such parameters as relative intensity distribution and (spatially variant) spatial resolution in the reconstructed image as well as and optimal geometric parameters for the read/write setups were derived. In addition, the selectivity of the system and cross-talk between multiplexed holographic images were estimated, and shown to be in agreement with experimental results [3].

1. We showed that information loss peculiar to the two-lambda hologram read/write technique can be circumvented using a multilayer recording medium [4]. We demonstrated theoretically and experimentally that such a system allows one to

significantly increase the storage density of the holographic memory without decreasing diffraction efficiency and/or increasing access time as compared to competing two-lambda systems.

2. We experimentally demonstrated multiplexed hologram recording in purple membrane BR-films, which until now (to our knowledge) has not been employed in a holographic memory system due to short life-time [2,3]. We showed that the properties of purple membrane BR-films admit two regimes of hologram multiplexing:

I. The hologram recording regime providing both long storage time (~5h) and low sensitivity (3-4J/cm^2) on the wavelength λ=633nm using for reading-out [3, 5].

The high sensitivity of the readout beam allows one to significantly increase the number independent accesses in optical memory systems without destroying stored information. Calculation shows that multiplexing 100 holograms per spot (2x2mm^2) (0.1 Gbit) in such a regime allows 10^4 readout operations (100 readouts of each hologram) with a decrease in DE of only 50%. This feature, along with the high value of the storage time, allows one to consider currently available purple membrane BR-film as an alternative recording material for constructing, e. g., cache-type memory systems.

II. Multiplexed holograms recorded in parallel and their selective reconstruction in real-time[2, 3].

This approach incorporates the modification of both angular and shift-multiplexing hologram encoding techniques along with an incremental exposure regime [4,5]. Holograms were recorded using an M-type recording regime of the BR. We experimentally demonstrated that by use of this technique one can circumvent the problems related to both short life-time of the M-state (2 min. for our films) and erasure of the holographic information during its readout. Thus, we were able to verify experimentally the calculated parameters of the optical memory using the short life-time M-state of the BR.

4. We considered the application of the BR (in particular multiplexed holograms recording in the BR) also for optical data processing.

- We demonstrated theoretically and experimentally that multiplexed holograms recorded in parallel can be used as an interconnection pattern reconfigurable in real-time. We presented the basic principles of such interconnections and estimated some of its parameters [3, 5].

- We showed that the technique of holographic parallel recording [2] can also be used for multichannel processing of optical signals allowing for significant increase of data throughput in pattern recognition systems [2].

- We demonstrated that the M-type hologram recording regime in the BR can be effectively used for constructing an optically addressable SLM [6]. This grating-type SLM is characterized by the following features:
  - high contrast
  - high sensitivity
  - a flexible transformation regime for optical signals which can be varied by changing the SLM parameters(relative intensities of the beams forming the active area of the SLM) to provide:
    - either a linear regime(for transformation of both binary and gray-scale optical signals);

Informal Report of Significant Findings

## submitted to Charles Gary, Program Monitor, October 1998

Nondestructive readout of the holograms recorded in a Bacteriorhodopsin

A. S. Bablumian, D. J. Mehrl, and T. F. Krile
OSL, Texas Tech University, Lubbock, TX 79409-3102
Octorber 21, 1998

We carried out two experiments examining the possibility of attaining non-volatile reconstruction of holograms recorded in purple-membrane BR-films.

The first approach is based on the idea that the quantum yield of phototransitions in BR depends on relative orientation of BR molecules and polarization of the light which launches the photocycle in BR. If this dependence is significant, then one can suppose that the hologram recorded in oriented BR-films can be reconstructed at the same wavelength without erasure using appropriate polarization of the readout beam. The experiment supporting this assumption was carried out using the setup depicted in the following figure:
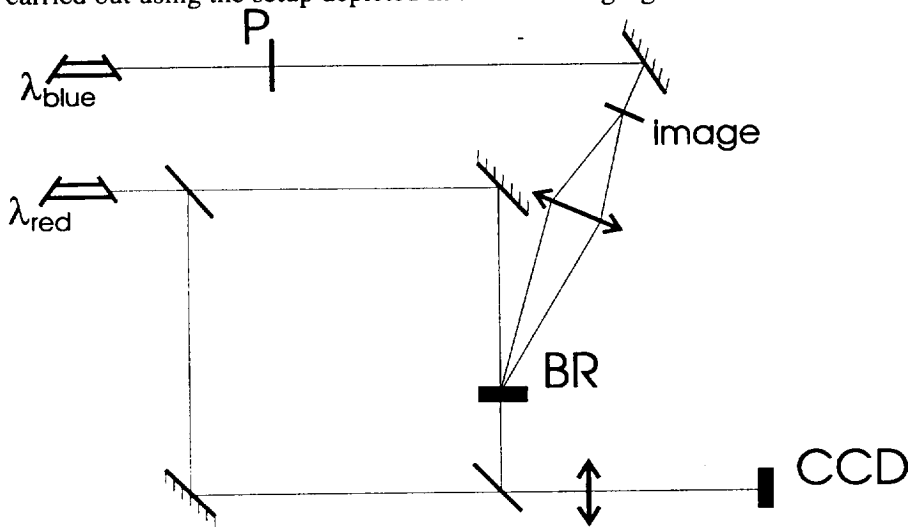
We project the blue image on the surface of BR-film constantly illuminated by red light and observe the modulation of the red light at different relative polarization orientations of the blue and red beams. To enhance the modulation contrast we employ a Mach-Zender interferometer geometry (see the figure) allowing us to subtract the 0-order component of the readout red beam and observe only its modulated part.

The images observed in these two polarization cases are presented in the next figure:

The difference between the image contrast was estimated to be as high as 5 times, and cannot be explained by induced anisotropy of the BR. If we assume that the modulation takes place in the M-type regime, then the most probable explanation is that red light selectively excites the BR

molecules having the appropriate orientation, and the back transitions of those excited BR molecules depends on the blue light polarization. The explanation of the low contrast image observed at orthogonal polarization can possibly be attributed to an alternative process where the blue light excites other BR molecules not previously excited out of the base state.

The investigation of the holograms recorded in BR in its initial state by blue light led us to results showing that the process cannot be considered as an M-type hologram recording. A hologram was recorded by blue and reconstructed by red light. We found that holograms recorded by only blue light and then reconstructed by red light have a life-time around 5 hours and very low sensitivity relative to red readout light(~3J). Illumination by the red light (readout process) brings the BR to the state where only the M-type regime predominates. The initial BR-state (i.e. erasure to ready the BR for new recording by blue light) is recovered by spontaneous decay in about two days, or by exposing to light with 380-400nm wavelength. In the following table we compare the parameters of holograms recorded by blue light before and after readout by the red light.

Exposure regime	Time	S	DE
Recording by blue light (λ<438nm) and then reconstruction by red light (λ=633nm)	5h	3J	3 - 5%
Illumination by red light before or during recording	2min	0.1mJ	4 - 8%*

* Varies with type of purple membrane film used.

The mechanism of this recording regime is not yet clear - apparently this is a Q-type regime which exhibits a behavior somewhat different from that described in the literature.

We are continuing the investigations, but even now the results are thought to make purple membrane BR-film an alternative material for constructing, e. g., cache-type memory systems. The figures in the table indicate that such a recording regime can provide a significant number of independent accesses in optical memory systems without destroying stored information. Calculation shows that multiplexing 100 holograms per spot (2x2mm^2) (0.1 Gbit) in such a regime allows 1000 readout operations with a decrease in DE of only 50%.

White Paper - submitted to NASA-Ames

August 10, 1998

A White Paper, submitted to NASA-Ames

by: A.S. Bablumian, D.J. Mehrl and T.F. Krile

August 10, 1998

BRIEF SUMMARY OF PROGRESS OVER THE LAST YEAR:

1.) We devised a simplified analysis/calculation scheme, based on coupled mode theory, for calculating critical parameters of our two-lambda holographic memory system. Our system[1], which used highly divergent spherical beams (via optical fibers) for both the reference and readout beams. Such parameters as relative intensity distribution, (spatially variant) spatial resolution, optimal parameters for the readout beam, and optimal geometric parameters for the reconstruction beam were derived. In addition, cross-talk between successive multiplexed holographic images was estimated, and shown to be in agreement with experimental results.

2.) We estimated the storage density achievable with BR-based holographic memory employing the aforementioned two-lambda technique, and suggested yet another multi-layer architecture[2] to allow an increase in storage density. We showed that this method afforded several advantages over rival methods, such as; (a.) increased selectivity without the partial loss of information inherent to two-lambda geometries, (b.) increased diffraction efficiency, and (c.) decreased access time.

3.) We investigated a hologram multiplexing technique employing both incremental recording and shift multiplexing, and showed that this hybrid approach allows one to multiplex (in parallel) a number of holograms within the same physical volume of the BR medium. We experimentally demonstrated that by use of this parallel recording technique the following optical BR-based memory systems can be realized:
     - Short-life-time BR films (purple membrane) can be used for holographic multiplexing. We recorded (10) holograms (each containing 1Mbit of information) in the same 0.01 square inch spot of the BR film, and selectively reconstructed all information contained in each hologram (using the two-lambda approach). The recording rate was 10Mbits/sec. Extrapolating on these parameters, we estimate a 36Gbit data capacity on a 6 x 6 inch BR disk.
     - The parallel multiplexing of point-source beams can provide the adaptive interconnection between 2-D arrays of lasers and photo-detectors (e.g. optical crossbar switches and multi-channel processing of optical signals).

4.) We experimentally demonstrated that the scattering noise of the BR, which limits the number of spatially overlapping holograms, can be significantly suppressed using filtering holograms, while having no detrimental effect on the reconstructed images.

PROPOSED FUTURE WORK

The previous results, along with the results of other preliminary experiments, lead us to suggest the following approaches (for future research) for significantly improving the performance of BR-based holographic memories.

1.) First, we plan on increasing the number of holograms that can be recorded within the same physical volume of the BR film (as mentioned above, we can currently record 10 holograms per

spot) and investigate the maximal attainable storage density in the BR-based optical modules. Our preliminary experiments showed the possibility of multiplexing 100 holograms per 2.5 x 2.5 (mm^2) spot on 100 micron thick BR film (using a 100ms exposure time), to attain 0.5 Tbit capacity for a 6 in. x 6 in. x 100 micron recording area.

In order to increase storage density, we would concentrate our effort in two directions:
- We would continue our investigation of the incremental recording technique. In particular, for recording 100 holograms in parallel it is necessary to significantly increase (temporal) switching frequencies between reference beams (we currently use an array of fiber-optic based reference beams) using, e.g. , a scanning mirror or an acousto-optic deflector.
- Reduce bit error rate during detection of weak signals by use of holographic filters to reject noise (see Fig. 1). We would investigate use of such filtering for a variety of recording geometries and recording materials.

2.) The properties of BR allow us to directly amplify weak optical signals. This feature could be exploited for the purpose of increasing the number of spatially overlapping multiplexed holograms (this increasing storage density). One of the possible approaches is based on the high spatial resolution of BR, and the fact that the state transition time is finite (~50 microseconds). Since absorption and refractive index varies significantly with states (e.g. between the M and BR states), the BR film can be exploited to act as a "trigger". First, we can increase the intensity of the image being detected using scale compression, i.e., demagnifying the image increases the intensity). The high spatial resolution of BR-films allows us to increase the intensity by at least an order of magnitude. Then, let us assume that a BR-film is continuously illuminated by a red light, which holds it in the excited M state. A (weak) reconstructed image, propagating on a blue light, is projected on the BR film surface, locally initiating the M $\rightarrow$ BR photo-induced transition. Simultaneously, the red light pushes BR molecules back to the excited M state. Naturally, the state transitions reach a steady state equilibrium, but the blue light image spatially modulates the BR film, also spatially modulating the (stronger) red light that ultimately is transmitted through the BR film. The red light, which now carries the (strengthened) image, can now be detected (in negative contrast) using, e.g., a CCD camera. Experimental results demonstrate the ability to detect weak optical signals in this manner.

An alternative approach is to "pump" the BR film with blue light, and modulate the BR with the image cast onto the BR surface using red light. In this case, we again obtain amplification, although the (amplified) output image (now with positive contrast) is now formed from the transmitted blue light. Experimental results show that this approach generally gives improved contrast ratio. However, disadvantages include the fact that silicon CCD detectors are generally less responsive to blue light than to red. In addition there are additional problems associated with the fact that some of the "intermediate" BR states are also photo-reversible.

In both cases, we employ the optical subtraction of the non-modulated part of the readout beam to increase image contrast. The amplification effect that we have observed could be enhanced significantly by the availability of thin films (~5 microns) having higher density of BR molecules.

3.) Normally, holographic memory systems simultaneously employ multiple read/write setups (for each layer), in order to enhance storage density (Figure 2a). This results in prohibitive cost and bulkiness of the system (e.g. requiring multiple SLMs, and/or CCDs etc.).

In order to reduce the cost of the system and make it more compact, we propose a wave-guide access scheme for reading and writing to a multilayer disk, that will use a common read-write access setup for all layers. The problem of selective recording and readout can be solved using reference and readout beams propagating in planar wave-guides placed between adjacent BR layers (see Fig. 2, 3a). A common write beam would be introduced into the wave-guides by
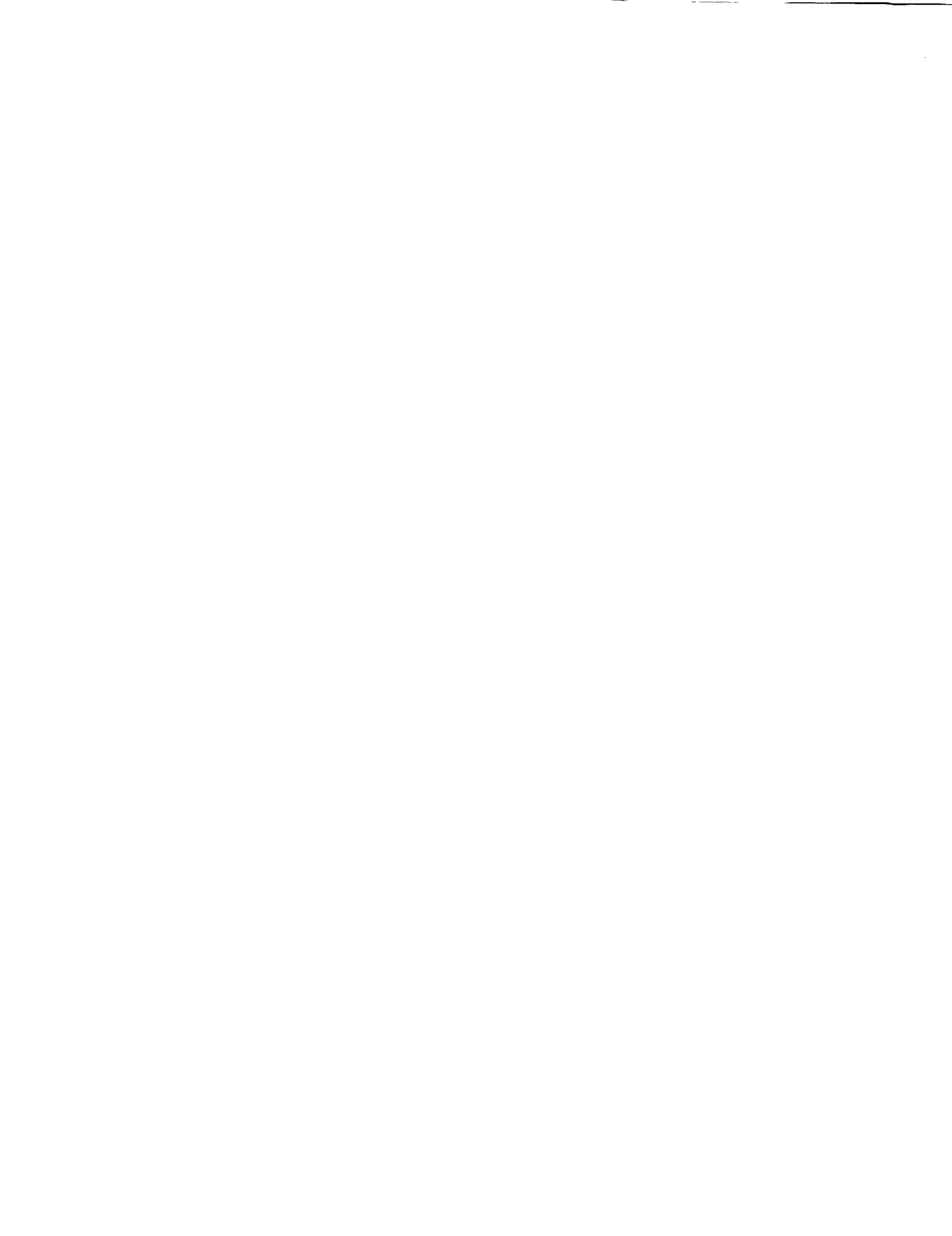
means of edge coupling for the input, and coupled via a surface grating for the output. A combination of spatial and phase multiplexing can also be employed to enable significant multiplexing within a given layer. The beams in the output of the grating G locally illuminate the particular spot of each BR layer where the holograms can be multiplexed using phase encoding methods. By rotating the multilayer medium relative to the stationary optical components (including the waveguide), we can spatially multiplex the set of phase-modulated holograms over the entire area of the recording layer.

Access to an individual layer (see Fig. 3b) is provided as follows: Each read/write beam is formed by one of the phase code holograms recorded on the rotatable disk D1, and coupled into the waveguide layer through its edge (see Fig. 3a). Figure 3b shows the recording geometry used to form a set of orthogonal phase code beams at the output of the grating (G). The interferometric mirrors, placed above each BR layer, have band-pass characteristics tailored to pass the reconstruction beam, while rejecting the readout beam.

This method, which incorporates phase encoded reference beams propagating in planar geometry, can potentially provide a significant boost in storage capacity. It would also be of interest to investigate alternative geometries for phase multiplexing. As a next step, we would investigate use of angular multiplexing, which can potentially provide even higher storage density.

OTHER IDEAS

1.) Optical networks: We have shown experimentally that the incremental recording of several point source beams at one wavelength forms , in real time, holograms which can effectively link , using a different wavelength, a particular laser source element (one of many in an array of point source elements) to a particular detector element (again, one of many detectors). The holograms are recorded on BR film using the M regime, in a way that the resulting optical interconnections are dynamically reconfigurable. Figure 4 illustrates, conceptually, the proposed interconnection geometry.

     Each laser and detector corresponds to a point on SLM1 and SLM2 respectively. Thus to establish, e.g., a one-to-one connection between N lasers and N detectors we need to find the corresponding pair of coordinates on SLM1 and SLM2, and expose the BR switching between these pairs in accordance with the incremental recording technique[1]. The address of the individual connection can be changed in real time (by changing the coordinates of the corresponding points displayed on the SLMs) during a time interval on the order of 50 microseconds (the time required for the BR $\rightarrow$ M state transition). In the same manner, one-to-many (broadcast) connections as well as many-to-one connections can be realized.

2.) We are planning to investigate the following features of BR films which potentially could provide hologram reconstruction without erasure.

- It is known that the change in refractive index due to the photo-stimulated transitions of BR states can occupy a BR volume several times larger than that of the BR molecule itself. Using this property, the following readout technique is proposed:

     A BR film is illuminated by an interferometric pattern form by two (blue) plane waves. Let us assume that we choose the period between the fringes to be less than the spatial resolution limit of the BR. A hologram is successively recorded using red light. Recording takes place only in the part of the BR film where the intensity of the interferometric pattern (formed by the blue light) is minimal. Thus the other areas (where blue light induced fringes are at non-minimal intensity) are excluded from recording with red light, as the blue light in those areas drives the BR back to the base (BR_0) state. Illumination of the BR molecules located in the areas of minimal (blue) intensity leads to a change of refractive index of the BR in an area that actually extends well out from the areas of minimal intensity due to the blue light interference. Hence, if one ot the blue beams is Bragg-matched with the hologram being recorded by red light, in this case the beam will effectively diffract the hologram without its erasure..

     Finally, another promising idea might allow nondestructive readout using BR films with oriented membranes. All current investigations are concentrated on fixing the data recorded in the excited M-state by applying an external electric field to the oriented BR molecules. It would be interesting to consider the opposite problem: investigate the decay of the sensitivity of the BR_0 (ground state) vs. applied electrical bias. If this effect is significant and we can "lock" the sensitivity of the BR, the following process of hologram recording/readout could be employed.

     A hologram is recorded using red (or yellow) light. Then, at the readout stage, and electrical bias is applied, which renders those areas of the BR that are in the BR_0 state relatively insensitive. Thus subsequent red light does not affect the initial state of the BR. At the same time the red light does not change the excited M-states (which are sensitive mainly to blue light wavelengths). Thus, upon reconstruction using red light, the red light will not erase the hologram. Of course, this approach would be practical only if the applied electric field does not dramatically alter the life-time of the BR (i.e. the thermal M $\rightarrow$ BR_0 transition).

Preliminary Budget Discussions:

Realizing the uncertainties in NASA funding, we anticipate that we would request a smaller budget. Because we have already acquired the necessary strategic capital equipment items necessary to conduct the proposed research (e.g., a precision motorized translation/rotation stages and a CCD equipped with an image intensifier), we would likely not need to request capital equipment in the upcoming proposal. In addition, we will not request secretarial support, would request a significantly reduced amount for office supplies, and would request reduced summer salary for the faculty involved (Drs. D.J. Mehrl and T.F. Krile). A significant portion of the budget would be dedicated towards providing salary for Research Associate A.S. Bablumian. It is anticipated that the budget request would be in the range of $80k to $85k.
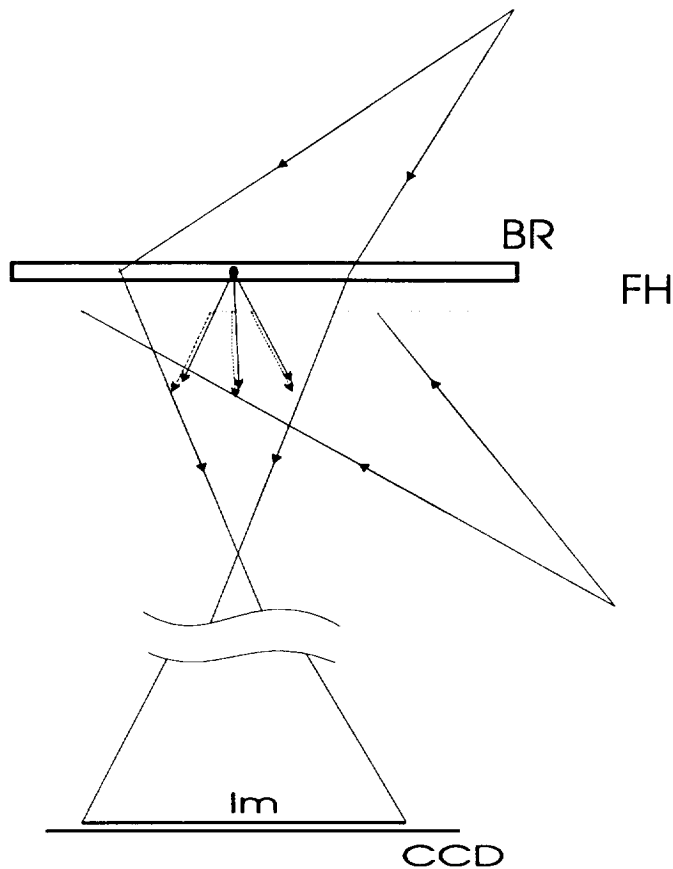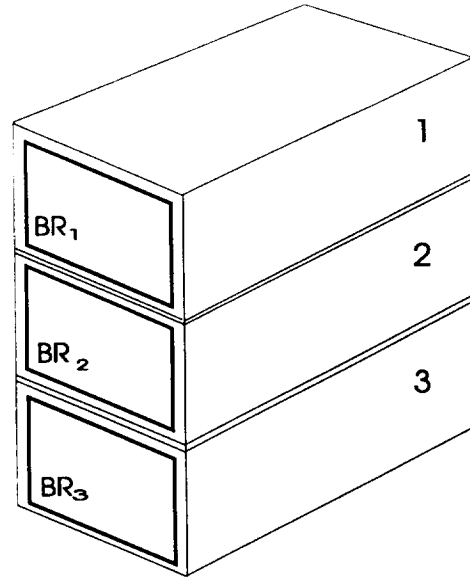
Fig. 1: Noise rejection during hologram reconstruction.
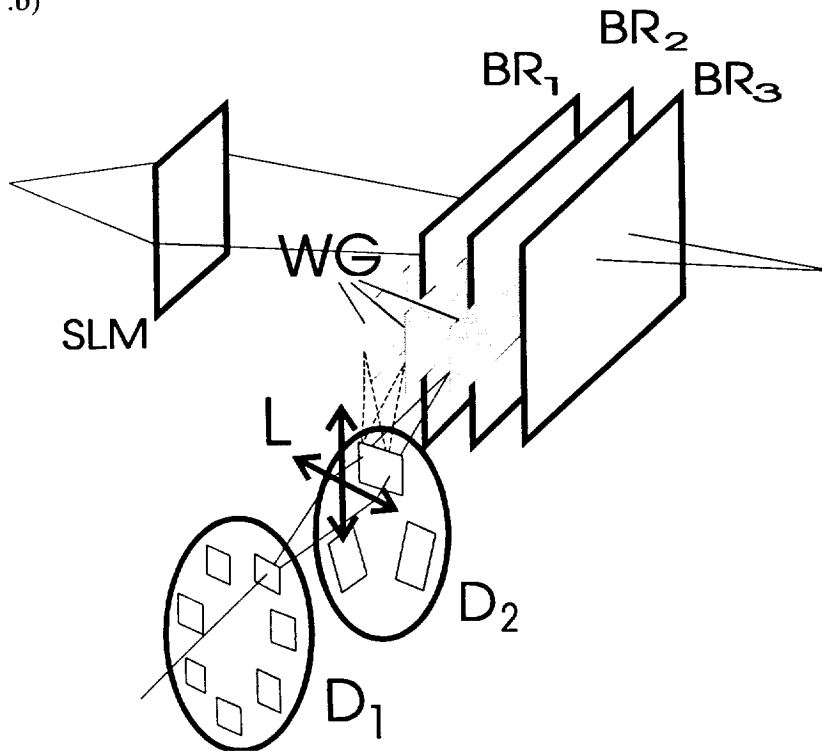BR, recording media; FH, holographic filter; Im, output image.

a)

.b)

Fig. 2: Holographic memory a) standard current setup; b) the setup with waveguide access scheme.
G, planar waveguide coupling reference beams with individual layer; D_1, rotatable disk with various phase code holograms; rotatable disk for selecting layers; L, focusing lens.
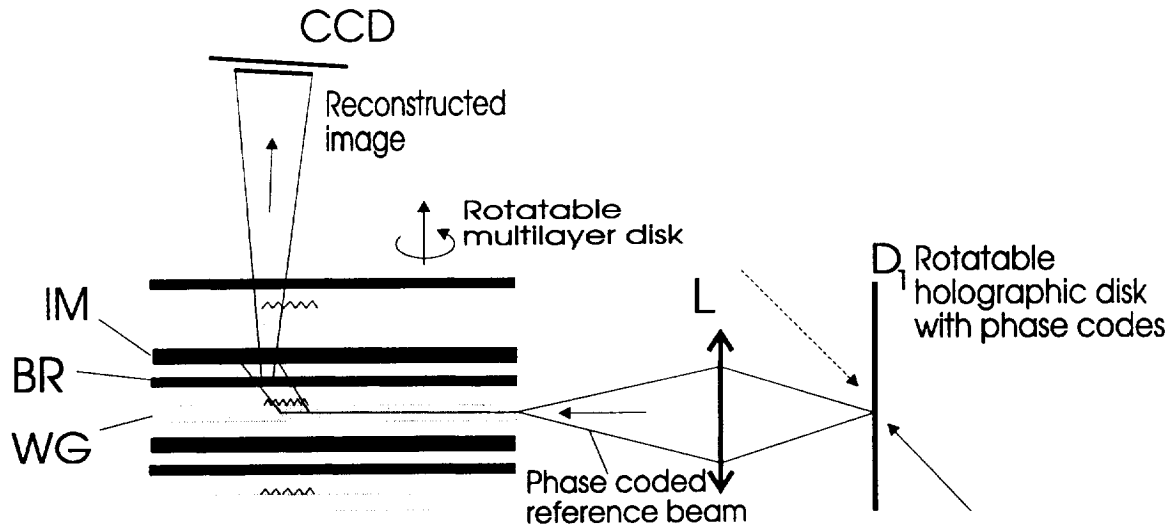
Fig. 3(a). Readout geometry with phase-coded reference beams.
IM, interferometric mirror; BR, recording layer; WG, planar waveguide with input-output grating.
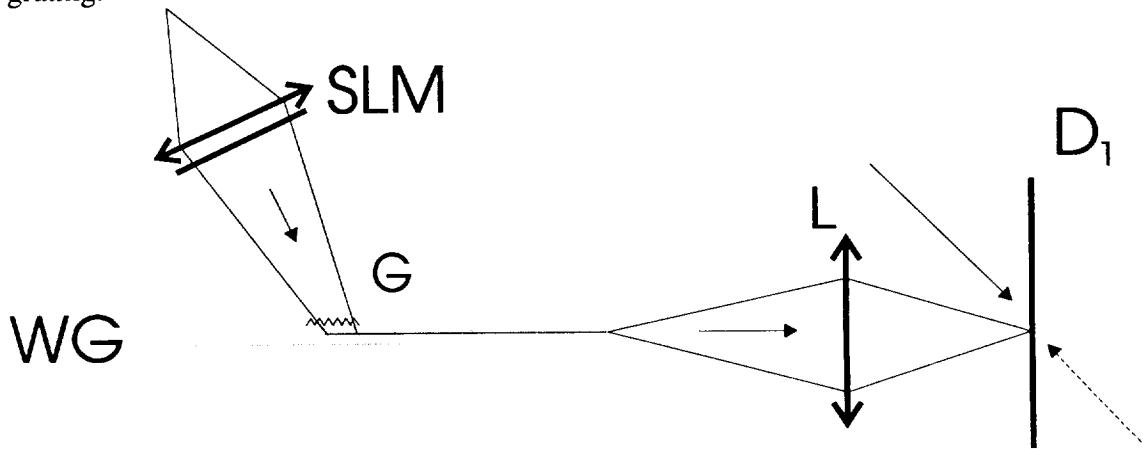

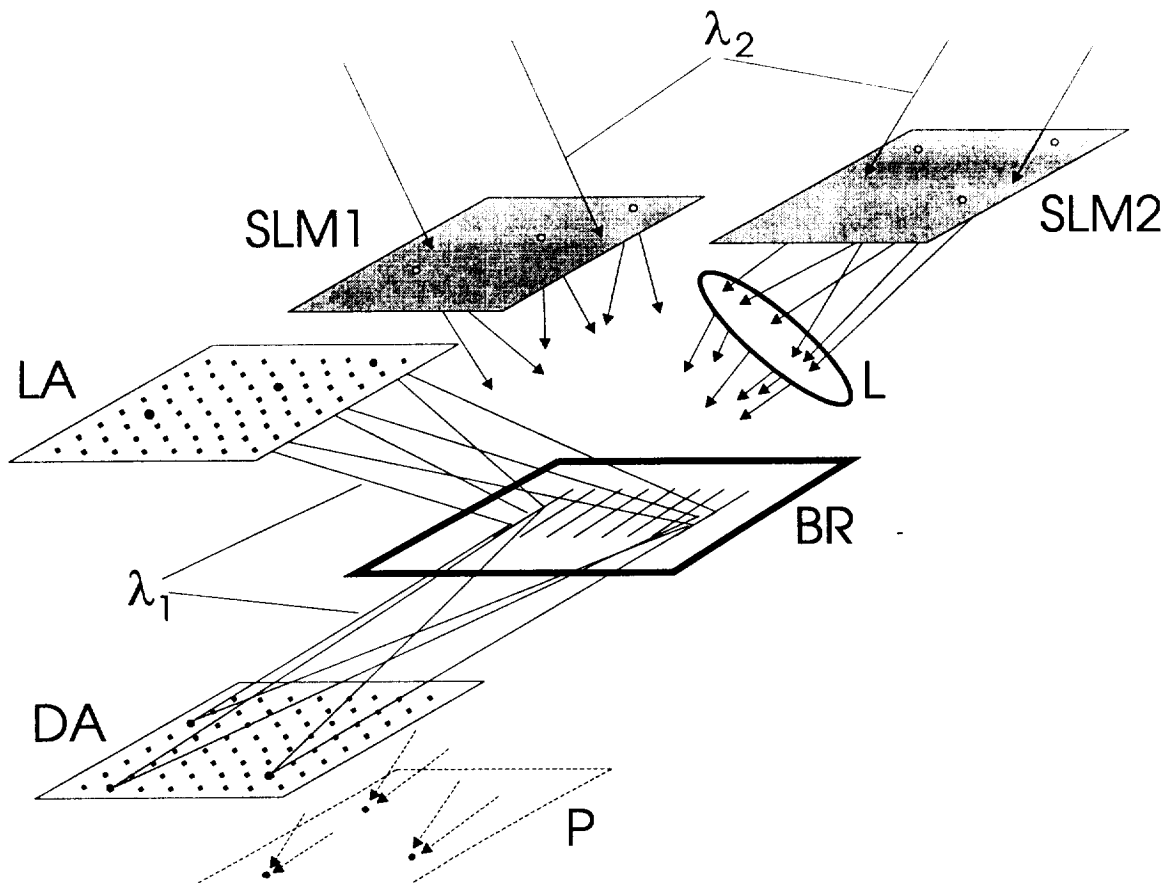Fig. 3(b): Recording geometry of holographic disk with phase codes (for one layer only).

Fig. 4: Optical network.
LA, lasers array; DA, detectors array; SLM1 and SLM2, spatial light modulators; L, projecting lens; P, image plane of the lens L.
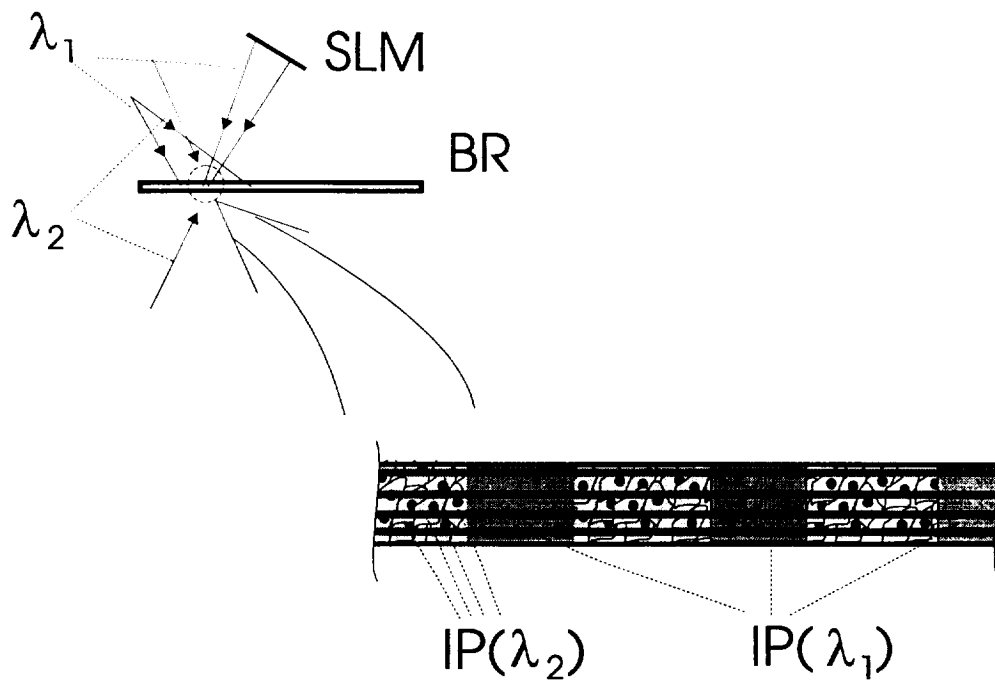
Fig. 5: The geometry of non-volatile reconstruction of hologram recorded in thick BR-film.

Power Point Presentation for Invited Paper at LEOS, '97

Presenter: David J. Mehrl

"Applications of Bacteriorhodopsin for Optical Data Storage and Processing," (*Invited paper - D. Mehrl presenter*), LEOS '97 Annual Symp. on Electro-Optic Sensors and Systems, (w. T.F. Krile, J.F. Walkup and A.S. Bablumian), San Francisco, CA (1997).

Programmable spatial filtering with bacteriorhodopsin

M. Storrs, D. J. Mehrl, and J. F. Walkup

We describe a programmable spatial-filtering system using bacteriorhodopsin (BR) film as a programmable, optically addressed spatial light modulator illuminated by a single wavelength of light. We use a computer-controlled mirror scanning system to write time-varying filter functions to the BR film and present proof-of-principle experimental results that demonstrate several elementary filtering operations. © 1996 Optical Society of America

Key words: Bacteriorhodopsin, spatial filtering, scanning systems, spatial light modulators.

1. Introduction

Fourier-plane spatial-filtering systems frequently suffer from a lack of flexibility, especially when standard photographic film is used as the spatial light modulator (SLM) bearing the filter function. Bacteriorhodopsin (BR) offers a flexibility not present with photographic film by serving as a reprogrammable, optically addressed SLM. A previous spatial-filtering system employing BR film and two wavelengths of light[1] exhibited a lack of flexibility in that the filter function was static. Our approach differs from previous systems by using a single wavelength of light and a computer-controlled, mirror-based flying-spot scanner to write the filter function to the BR film. We exploit the retention properties of the BR film to make scanning a feasible technique. Taking advantage of the photocycle of BR film allows us to update the filter function. This arrangement combines the optical advantages of BR films with the simplicity of scanning systems to achieve a flexible spatial-filtering system.

BR film contains the photochromic protein bacteriorhodopsin found in the purple membrane cell wall of the salt-marsh bacterium, Halobacterium halobium.[2] The protein molecules are extracted from the bacterial cell and deposited on an optically flat substrate. The BR molecule is characterized by cyclical photochromic changes. The BR molecule has a characteristic wavelength-dependent photoabsorption profile for each of the molecular states in its photocycle. A simplified depiction of the BR photocycle[2] is shown in Fig. 1. The BR molecule is initially in the BR state and has an absorption maximum at 570 nm. At illumination by light of a wavelength near the absorption peak, the BR molecule undergoes a rapid (~3-ps) photoinduced transition from the BR state to the short-lived (~1-μs) intermediate K state. BR then undergoes a rapid (~50-μs) thermal relaxation to the M state in which it has an absorption maximum at 410 nm. The M state is relatively long lived, with a lifetime dependent on the relative humidity and pH of the environment in the manufacturing of the films[3] and can vary from a few milliseconds to hours. The films used in our experiments had M-state lifetimes of approximately 10 s. The molecules in the M state transition back to the BR state through thermal relaxation. As an alternative, the molecules in the M (410-nm) state can be forced back to the BR (570-nm) state by the absorption of light near the second wavelength (410 nm). This provides an effective method to erase the films. The absorption spectra of the various photocycle states[4] are shown in Fig. 2. Note that the absorption peaks for the BR and M states are shifted with respect to each other, although there is a significant overlap.

BR holds promise as a SLM because of its high sensitivity (typically 30–80 mJ/cm^2), rewritability (more than 1×10^6 cycles without observable degradation),[5] fast response (typically 50 μs),[6] high spatial resolution (exceeding 5000 lines/mm)[7] because of the small molecule size, long-term physical and chemical stability, and ease of manufacture.[8]

The authors are with the Optical Systems Laboratory, Department of Electrical Engineering, Texas Tech University, Lubbock, Texas 79409-3102.
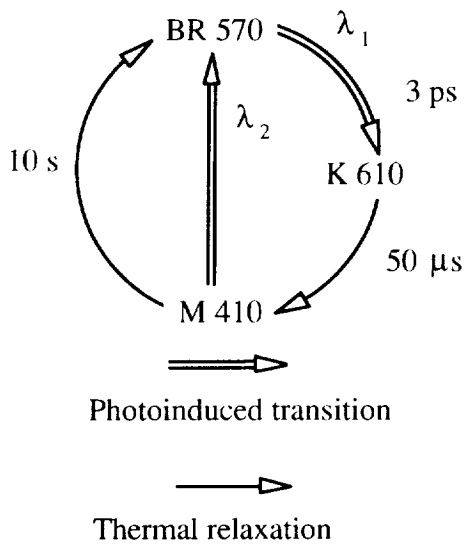
Fig. 1. Simplified depiction of the photocycle for bacteriorhodopsin.

Fig. 3. Schematic diagram of the dynamic spatial-filtering system.

At constant illumination with light of a single wavelength (e.g., 514 nm, one of the predominate lines of an argon-ion laser), the BR molecules undergo a photoinduced transition from the BR state to the M state, and simultaneously molecules in the M state transition to the BR state through both thermal relaxation and photoinduction. A steady-state population of molecules in the M state is quickly achieved (because of the 50-μs response time), and the absorption (and consequently the local intensity transmittance) of the BR film takes on a value dependent on the intensity of the incident illumination. The intensity-dependent transmittance of a thin BR film can be described by[1] $\tau(I) = \exp[-\alpha(I)d]$, where τ is the local intensity transmittance of the BR film, $\alpha(I)$ is the intensity-dependent local absorption coefficient, and d is the thickness of the film. Illuminating the BR film with a relatively intense write beam allows the resulting intensity-transmittance pattern to be used as a SLM for a less intense object beam.

Scanning systems offer high spatial resolution, economy, and convenience when compared with costly SLM's. The relatively long retention time of our BR films (~10 s) provides ample time for our mirror-based scanning system to write a complete filter pattern to the BR film. Time concerns can be further alleviated by the use of a high-speed scanning system, such as an acousto-optic (AO) scanning system.

The BR film also undergoes local changes in the refractive index on illumination.[9] This spatial refractive-index distribution will, in general, modify the system output; however the filter functions we wrote to the film were binary in nature, so the trans-
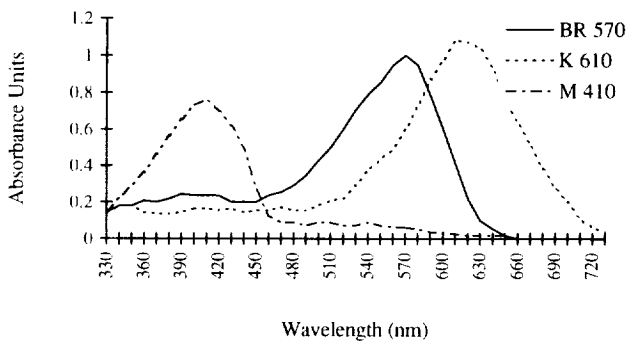

Fig. 2. Absorption spectra of the intermediate states in the photocycle of bacteriorhodopsin: BR 570, BR state at 570 nm; K 610, K state at 610 nm; M 410, M state at 410 nm.
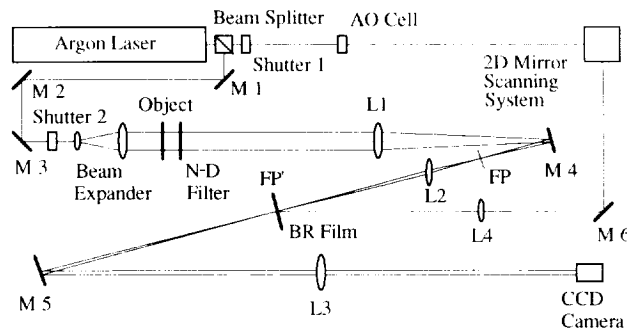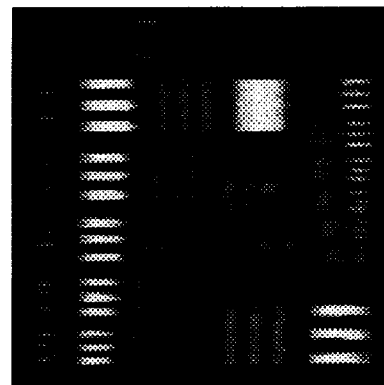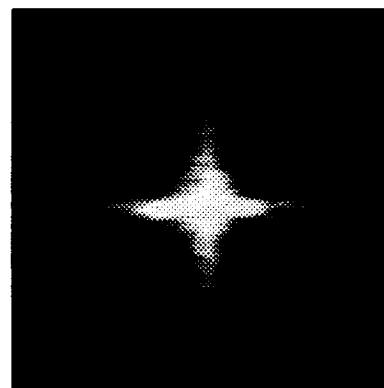

(a)

(b)

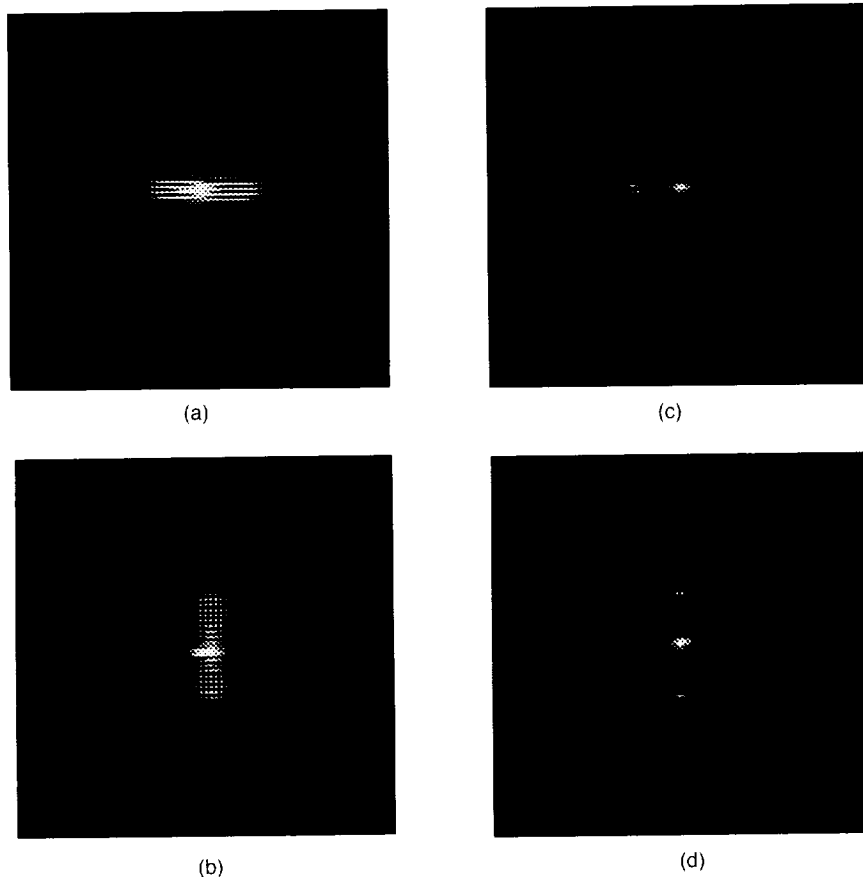Fig. 4. Images of (a) the test object and (b) its Fourier transform.

Fig. 5. Filter functions demonstrating dynamic spatial filtering with (a) a directional low-pass filter highlighting vertical elements, (b) a directional low-pass filter highlighting horizontal elements, (c) a directional bandpass filter emphasizing vertical elements, and (d) a directional bandpass filter emphasizing horizontal elements.

mitted object beam experienced a constant phase shift.   Consequently the effects of refractive-index variations could be neglected in our experiments.   In a system in which continuous filter functions are written to the BR film, additional analysis may be required to assess the effects of the resultant phase modulations.

2. Experimental Setup

The proof-of-principle dynamic spatial-filtering system we investigated is shown in Fig. 3.   An argon-ion laser beam, operating at the 514-nm line and at approximately 50 mW, with a beam diameter of approximately 1.3 mm, was split into an object beam and a filter write beam.   A pair of shutters are included to block the filter write beam and the object beam between experimental runs.   The expanded beam illuminating the input object was passed through a neutral-density (N-D) filter with an optical density of 2 to produce a low-intensity object beam, so as to minimize the relative transmittance changes it produces in the BR film.   The object beam was applied continuously throughout the run of the experiment.   Lens L1 (f = 910 mm) forms the Fourier transform of the object at the plane marked FP.   For convenience we positioned lens L2 (f = 150 mm) to

magnify the Fourier distribution of the object at the plane marked FP' by approximately a factor of 4. We placed the SLM bearing the filter function at this plane to pass the desired frequency components of the input object selectively.   Lens L3 (f = 910 mm) images the filtered object beam onto a CCD camera that serves to record the resulting filtered and demagnified (by approximately a factor of 0.25) image.   A frame grabber was used to record a single frame of the CCD camera image.

The filter function was written to the BR film by a computer-controlled scanning system.   An AO cell was positioned in the filter beam to serve as a high-speed shutter by deflecting the filter beam into the two-dimensional (2D) mirror-based scanning system. In a more sophisticated system the AO cell could also serve to amplitude-modulate the intensity of the filter write beam.   Filter functions were written dynamically to the BR film, and we relied on the film's thermal relaxation to erase the filter.   In our experiments the filter write beam was positioned at an angle with respect to the object beam.   This provided the advantage of simultaneous exposure of the BR film to the object beam and to the filter write beam without exposure of the CCD camera to the intense filter write beam.   Lens L4 (f = 500 mm) is
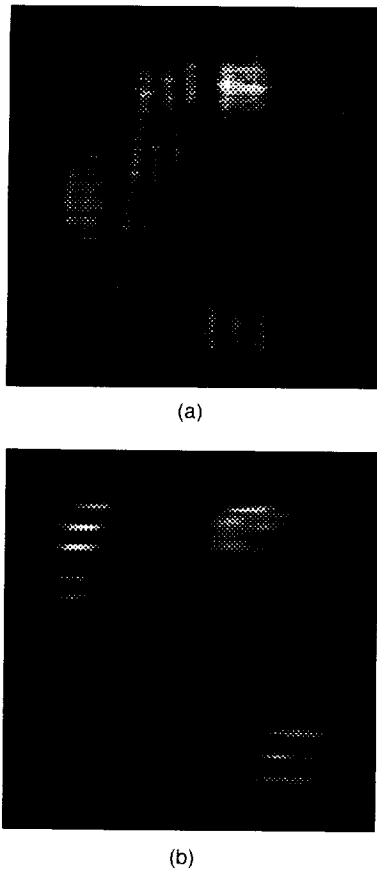
(a)

(b)

Fig. 6. Filtered images obtained by the use of (a) a vertical-element pass filter and (b) a horizontal-element pass filter.

positioned to demagnify the spot diameter in the FP' plane by a factor of approximately 0.25. The write-beam spot diameter was approximately 0.3 mm. The energy density used in the filter write beam was approximately 10 mJ/cm².

The test object chosen for our proof-of-principle experiments was a U.S. Air Force resolution-test-chart pattern consisting of vertical and horizontal stripes at varying spatial frequencies. The test mask has an overall aperture of approximately 12 mm and spatial frequency components ranging from 1 line pair/mm to 228 line pairs/mm. The Fourier transform of this object lies primarily along the vertical and horizontal axes in the Fourier plane. We took advantage of this fact in choosing the filter functions to be written to the BR film. The object and its Fourier spectrum are shown in Figs. 4(a) and 4(b), respectively. The blurring seen in Figs. 4 is largely an artifact of the frame grabber. The enlarged central portion of the Fourier spectrum in Fig. 4(b) is a result of blooming in the CCD camera.

The filter functions chosen to demonstrate dynamic spatial filtering were directional low-pass and band-pass filters. We implemented the directional low-pass filters by writing a transmissive stripe to the BR film along either the vertical or horizontal axis in the Fourier plane. This filter function serves to empha-

size either the horizontal or vertical elements, respectively, of the object and to low-pass-filter the remaining elements. We obtained the directional bandpass filter by writing a pair of spots to the BR film on the vertical or horizontal axis in the Fourier plane and locating them symmetrically with respect to the center of the Fourier plane. This filter serves to emphasize either the horizontal or vertical elements of the object at the spatial frequencies specified by the distances of the spots from the center of the Fourier distribution. These filter functions were selected for their ease of implementation and are shown in Figs. 5 superimposed on the Fourier spectrum of the object. Because of the relative intensities of the object and the filter write beams, only the central portion of the Fourier spectrum is visible in these figures. Striations in the images are largely video artifacts from the frame grabber.

An arbitrary filter function may be written to the BR film if the filter beam is scanned across the BR film and the intensity of the filter beam is modulated. This written function may be achieved if the mirror system is moved so as to scan the write beam in a tight spiral, thus minimizing abrupt mirror translations and continuously modulating the intensity of the beam with an AO cell.

3. Experimental Results

Experiments were conducted with a time-varying directional filter that alternately emphasized the vertical and horizontal elements of the object. Single frames of the results obtained with both filters are shown in Figs. 6. For presentation purposes the contrast of the images has been maximized. We observe from Fig. 6(a) the enhanced vertical stripes and the blurred horizontal stripes of the test object that result from low-pass filtering. From Fig. 6(b) we observe the enhancement of the horizontal elements of the object and blurring of the vertical elements, again resulting from low-pass filtering. Dynamic filtering was demonstrated by the alternate application of the vertical-element filter for approximately 1 s; this was immediately followed by the application of the horizontal-element filter function for approximately 1 s.

Additional experiments were conducted by use of an alternating bandpass filter that was also dynamically altered to pass decreasing spatial frequencies. This dynamic alteration serves to emphasize the object's vertical and horizontal elements of decreasing spatial frequencies alternately. A time sequence of these results is shown in Figs. 7. The images in Figs. 7 were captured under the same conditions, and the relative increase in brightness for different spatial frequencies is due to spatial filtering. For presentation purposes the contrast of the images has been maximized. In Figs. 7(a) and 7(c) the effects of a vertical-element bandpass filter of varying spatial frequencies is demonstrated. In each of these figures the horizontal elements of the test object are blurred and the vertical elements of the spatial frequency that was specified by the filter function are
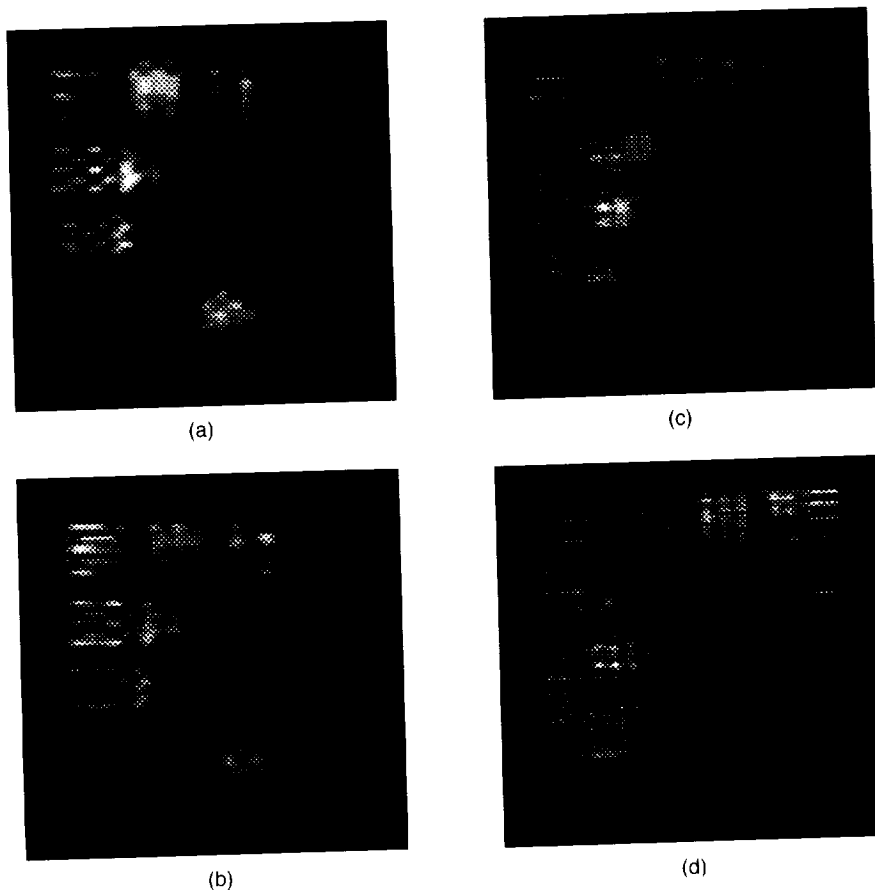
Fig. 7. Filtered images obtained with bandpass filters of differing spatial frequencies: (a) and (c) show vertical-element filtered images and (b) and (d) show horizontal-element filtered images.

enhanced.   Figures 7(b) and 7(d) illustrate the effects of horizontal-element bandpass filters of varying spatial frequencies. Figure 7(d) shows horizontal elements of a higher spatial frequency emphasized in the upper right-hand corner of the image; Fig. 7(c) shows vertical elements of a higher spatial frequency emphasized in the middle left-hand portion of the image. Figure 7(b) shows horizontal elements of a lower spatial frequency in the upper left-hand corner of the image; Fig. 7(a) shows vertical elements of a lower spatial frequency emphasized in the upper center portion of the image.   Dynamic filtering was demonstrated by the alternating application of vertical and horizontal bandpass filters (again, each filter was applied for approximately 1 s) and the selection of progressively lower spatial frequencies by means of decreases in the distance between the spot pairs.

4. Conclusion

In summary, the use of BR films in conjunction with a scanning system has been demonstrated as an optically addressed spatial light modulator in a programmable Fourier-plane spatial-filtering system. Experiments have demonstrated several elementary filtering operations.

References

1. R. Thoma, N. Hampp, C. Bräucle, and D. Oesterhelt, "Bacteriorhodopsin films as spatial light modulators for nonlinear-optical filtering," Opt. Lett. **16,** 651–653 (1991).
2. D. Oesterhelt, C. Bräuchle, and N. Hampp, "Bacteriorhodopsin: a biological material for information processing," Q. Rev. Biophys. **24** (4), 425–478 (1991).
3. O. Werner, B. Fischer, A. Lewis, and I. Nebenzahl, "Saturable absorption, wave mixing, and phase conjugation with bacteriorhodopsin," Opt. Lett. **15,** 1117–1119 (1990).
4. Z. Chen, A. Lewis, H. Takei, and I. Nebenzahi, "Bacteriorhodopsin oriented in polyvinyl alcohol films as an erasable optical storage medium," Appl. Opt. **30,** 500–509 (1991).
5. R. Hampp, R. Thoma, D. Oesterhelt, and C. Bräuchle, "Biological photochrome bacteriorhodopsin and its genetic variant Asp96 → Asn as media for optical pattern recognition," Appl. Opt. **31,** 1834–1841 (1992).
6. J. Downie, "Real-time holographic image correction using bacteriorhodopsin," Appl. Opt. **33,** 4353–4357 (1994).
7. C. Brächle, N. Hampp, and D. Oesterhelt, "Optical applications of bacteriorhodopsin and its mutated variants," Adv. Mater. **3,** 420–428 (1991).
8. R. Birge, "Protein-based optical computing and memories," Computer **25,** no. 11, 56–67 (1992).
9. Q. Song, C. Zhang, R. Gross, and R. Birge, "Optical limiting by chemically enhanced bacteriorhodopsin films," Opt. Lett. **18,** 775–777 (1993).

M-type thick holograms in bacteriorhodopsin films with a high-divergence reference beam

Arkady S. Bablumian, Thomas F. Krile, David J. Mehrl, and John F. Walkup

The capacity to use differing read and write wavelengths for reconstructing volume holograms recorded in a shift-multiplexing geometry is analyzed and realized for M-type volume holograms recorded on bacteriorhodopsin films. The intensity distribution in the reconstructed wave is calculated as a function of the parameters of the recording and readout beams. Optimal recording and retrieving geometries, as well as a precise method for tuning the readout setup, are suggested. © 1998 Optical Society of America

OCIS codes: 090.0090, 090.7330.

1. Introduction

High-capacity storage of optical information can be achieved by holographic recording throughout the volume of a thick medium.[1] The strong sensitivity of thick holograms to the parameters of the reconstruction beam allows one to multiplex many holograms in the same volume and then read them out selectively. The simplest way to retrieve any desired hologram is to use a readout beam identical in all respects to the reference beam used for recording. At the same time, for nondestructive retrieval of stored holograms it is necessary either to fix them or to reconstruct them at wavelengths to which the material is insensitive. (The latter is of particular interest in the general area of real-time optical data processing.) In general, changing the readout wavelength will change not only the output's orientation (in accordance with the Bragg condition) but also the shape of the wave front. This leads to both a loss of information in the object beam and difficulties associated with the synthesis of a readout beam with a complicated wave-front shape.

Hologram reconstruction with different wavelengths that employs distortion compensation during reconstruction by means of changing the curvature of the readout wave front was described in Ref. 2. In the paraxial approximation using the coupled-wave theory, the authors calculated the optimal parameters for the readout beam (focal length) and assessed the width of the reconstructed spherical beam. Unfortunately, under the approximations used in Ref. 2 this approach cannot be applied for analyzing several interesting hologram-multiplexing geometries for situations in which recording beams are highly divergent spherical waves. Such a geometry was investigated in Ref. 3, which described a hologram of an information-bearing signal considered to be a superposition of plane-wave elemental holograms with the same spherical reference beam. The plane-wave object beam of each elemental hologram represented a single component of the signal. This approach allowed the authors to calculate the optimal parameters of the reconstructing beam—a shift parameter characterizing hologram selectivity—and an assessment of maximal resolution in the reconstructed image.

In this paper we apply another approach in which we consider the relative change of the intensity distribution in the frequency plane of the signal. For an arbitrary wavelength we calculate the reconstruction of the points of the Fourier transform of a signal by considering the hologram as a superposition of elemental holograms, each being formed by two point sources. We show that, besides the parameters mentioned above, such an approach allows one to assess distributions of both relative intensity and resolution along the reconstructed image. These parameters are then compared with values derived experimentally.

It is necessary to note that the readout beam has to be calculated and oriented with respect to the hologram with high accuracy, according to the shift se-
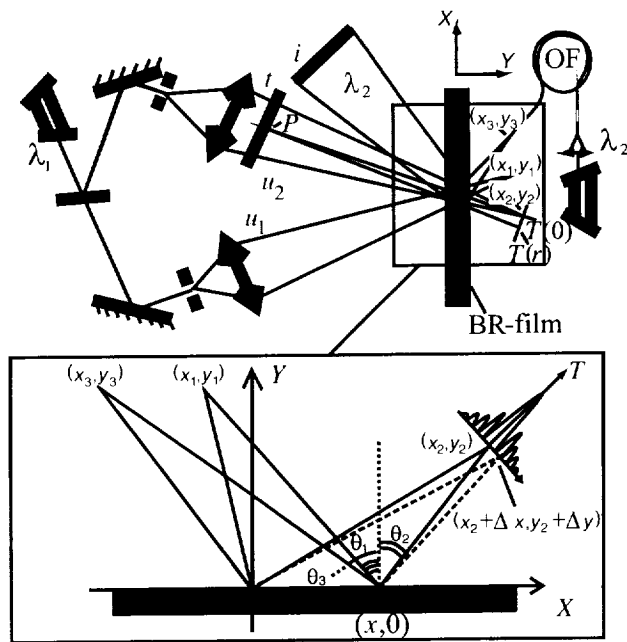
Fig. 1. Geometry of the recording and readout rays. Here t and T denote the transparency and its scaled Fourier transform, respectively, i represents the reconstructed image, and OF denotes the optical fiber.

lectivity of a chosen setup.[3] Since the orientation has three degrees of freedom and recording beams have to be measured with the above-mentioned accuracy, it becomes clear that the results cannot be applied easily without some practical method of finding the optimal location of the readout beam. So our next step was to develop a method for tuning the readout setup. Finally, experimental verification of the theory is demonstrated by use of M-type holograms in bacteriorhodopsin (BR) films.

2. Theory

Let the hologram be recorded by the reference u_1 and object u_2 waves, as shown in Fig. 1. In both recording arms the laser beams are expanded and then point focused. This allows both the formation of a spherical reference beam and the insertion of the information into the object arm by use of a transparency with transmittance t. The scaled Fourier transform of t is produced at the plane of the beam focus [(x_2, y_2) in Fig. 1]. Here we let (x_1, y_1) designate the coordinates of the spherical reference source and (x_2, y_2) designate the coordinates of the zeroth-order component of the Fourier spectrum of transparency t.

The hologram of transparency t can itself be regarded as the superposition of an array of elemental holograms, each being formed by a pair of spherical beams whose sources are located at the point (x_1, y_1) and one of the points of the Fourier plane [$(x_2 + \Delta x, y_2 + \Delta y)$ in Fig. 1]. The hologram of the zeroth-order component of the Fourier spectrum T [$H(\Delta x, \Delta y) = H(0, 0)$] will determine the background in the reconstructed image I, whereas the holograms of higher-

order components [$H(\Delta x, \Delta y)$] will determine its resolution. It is evident that each elemental hologram can be reconstructed by the beam whose parameters coincide with those of one of the recording beams. The existence of reconstructed beams whose wavelengths differ from the recording wavelength becomes clear from the following: Each elemental hologram is recorded by point-source beams; therefore any of its small parts is described by the constant grating vector K. This means that, for an arbitrary wavelength λ in every point (x, y) of the elemental hologram, two rays (incident and diffracted) oriented at the Bragg angle to the grating vector K are determined unambiguously. The lattice of rays combines to form only two beams that can be diffracted by this hologram and that, generally speaking, for an arbitrary wavelength λ are not spherical.

Let us consider hologram reconstruction by a spherical wave u_3 with coordinates (x_3, y_3) and determine the Bragg mismatch angle δ for its rays at every point of their crossing within the hologram. Let us also consider the cone of rays emanating from (x_3, y_3) with an average spatial frequency β_k. The angular aperture of this cone of rays we choose is small enough to consider it to be a plane wave. Our purpose is to define the conditions under which (1) the intensity change along the cone in hologram H is equivalent to (2) the intensity change of a plane wave incident on a plane diffraction grating. Such an analogy will allow us to assess the diffraction in the case 1 by calculation of the diffraction in case 2 in accordance with the coupled-wave theory.[4] Under suitable approximations, described below, the intensity of the plane wave in the output plane of the equivalent diffraction grating will be equal to the output intensity of the cone of rays. Continuing this procedure for all β_k, we can calculate the output intensity arising from the source u_3. Then one can calculate the intensity distribution of the diffracted beam for each elemental hologram H, considering the sum of the incident and diffracted beams to be constant. The sum of the elemental holograms corresponds to the Fourier spectrum of the transparency T, by which we can estimate the resolution in the reconstructed beam.

First, let us consider the main arguments supporting the proposed approximation, as well as the limits of its applicability. The diffraction process is determined mostly by the direct energy diverted from the incident into the diffracted beam when the values of the diffraction efficiency (DE) are low (typically the case for BR). It follows from the fact that the amplitude change of the incident wave is proportional to the amplitude of the diffracted wave, and vice versa, that the amplitude change of the diffracted wave is proportional to the amplitude of the incident wave.[4] Therefore the diverted energy proceeds mainly in one direction when the difference between the amplitudes of the interacting waves is large. Let us neglect the influence of the parameters of the diffracted beam on the intensity change of the incident beam. This assumption and the fact that the incident rays
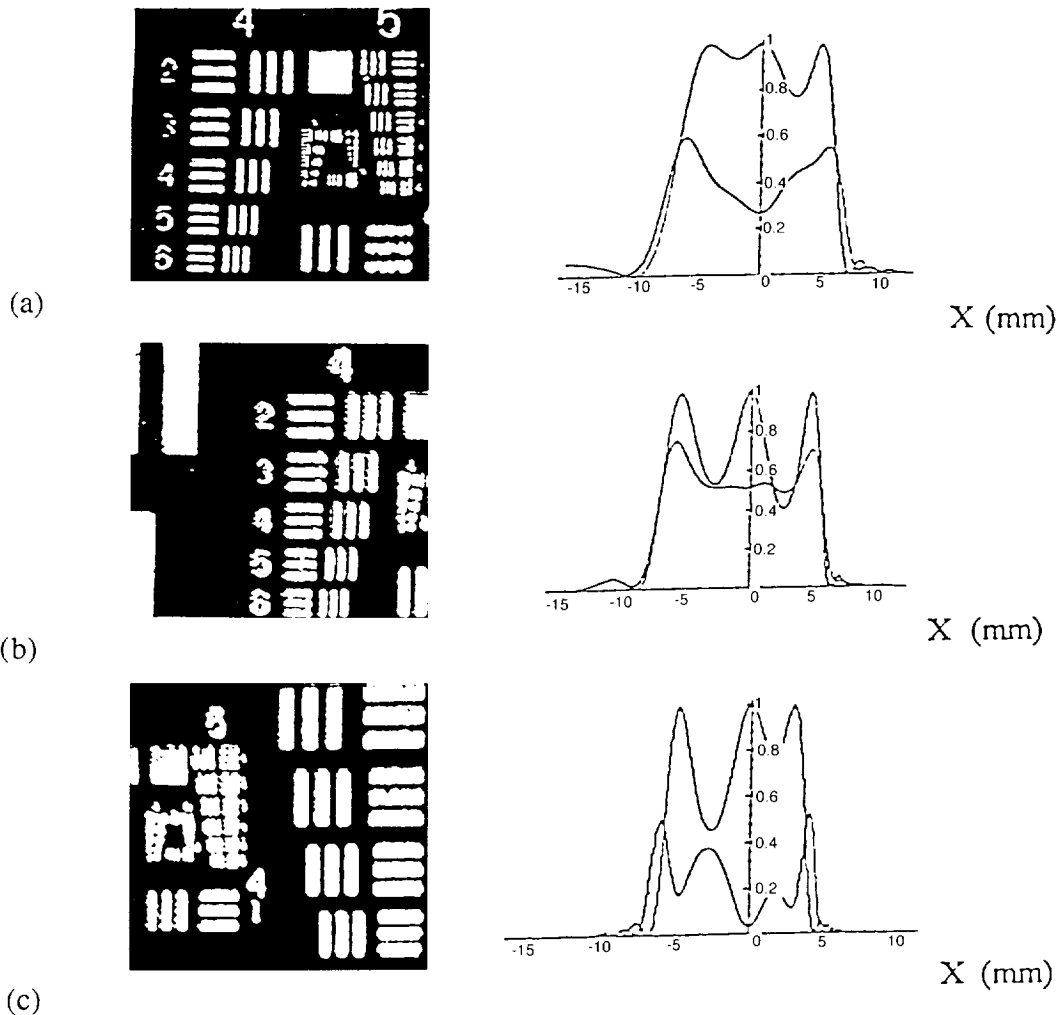
(a)

(b)

(c)

X (mm)

Fig. 5. Photographs of transparency t from hologram H and the corresponding plots of reconstructed beams from two elemental holograms, $H(r = 0)$ (upper traces) and $H(r = 1$ mm) (lower traces), in the exit plane of hologram H for (a) $Q = 100$, (b) $Q = 300$, and (c) $Q = 750$.

molecules, transforming them into the M-state ready for recording with blue light. Using M-type holograms allowed us to investigate the two-lambda method[3] of constructing the holographic memory and, simultaneously, to change and compare in real-time the recording and readout parameters.

Mutant variant BR_{D96N} films with a thickness of 100 μm were used. A hologram of a standard U.S. Air Force test pattern was recorded at $\lambda = 458$ nm and reconstructed at $\lambda = 633$ nm. The setup geometry for recording and reconstruction was chosen according to the theory described in Section 2, enabling us to compare the experimental results with the results derived theoretically (see Figs. 2–4).

As was pointed out above, in a recording regime with a high sensitivity to shift the process of finding the location of the readout beam with the given parameters becomes a difficult problem practically. This is particularly true for high values of the Klein parameter Q. For optimally tuning the readout setup the following method was suggested and utilized: The thick recording medium was first re-

placed by a structure consisting of two separated thin films. A hologram recorded in such a structure, in contrast to a common thick hologram, can be reconstructed by readout beams of any orientation. This forms two images that are propagated, in general, in different directions. On optimal orientation of the readout beam these directions coincide, and interferometric fringes of overlapped images coalesce into one fringe. From the maximal size of this fringe one can judge the accuracy of the reconstruction source location.

For modeling the volume medium a 1-mm glass plate with photoresist layers on both surfaces was used. The readout beam was formed by use of a piece of optical fiber to facilitate precise positioning of the point source. After finding the optimal position for the reconstruction source, we then replace the model medium with the BR film. We also devised a technique (not discussed here for the sake of brevity) to compensate for the fact that the overall thickness of the model medium and the BR film are not the same.

Figure 5 presents photographs of the U.S. Air Force test-pattern image reconstructed from the BR film with different values of the Q factor. For comparison, next to each photograph we show plots of the intensity profiles of beams diffracted from two elemental holograms, $H(0, 0)$ and $H(r = 1$ mm$)$, recorded in the corresponding geometry. As was pointed out above, a sufficient DE for these two elemental holograms automatically ensures a sufficient DE for all elemental holograms $H(|r| \leq 1$ mm$)$ (remember that r is the coordinate in the frequency domain). With the parameters of the beam u_2 taken into account, it is easy to calculate that the reconstruction of a 1-mm-extent u_2 in the frequency plane provides a 30-μm resolution in the reconstructed image [Eq. (2.7)]. As one can see, this resolution (the width of the first element in the fourth group of the test pattern), which conforms to the lower traces in Figs. 5(a)–5(c), is provided over all the field of the reconstructed image for $Q = 100$, 300 but is reduced for $Q = 750$. These results are supported by analysis of the corresponding photos. The experimental sensitivity of the setup with $Q = 750$ to the shift of the readout beam was approximately 20 μm, deviating by 5%–6% from the theoretical prediction. The measured DE of the reconstructed images was approximately 4%–5%.

4. Conclusions

We have demonstrated a relatively simple method of calculating critical parameters for the processes of reading and writing volume holograms using highly divergent beams of differing wavelengths. The experimental results were shown to agree with the theoretical results. We have considered the resolution and relative-intensity distribution of the reconstructed image stored in a thick hologram by a high-divergence reference beam that is arbitrarily oriented relative to the object beam. These param-

eters, as well as the optimal parameters of the readout beam, can be estimated from the intensity profiles of beams diffracted by two elemental holograms (recorded by a pair of spherical beams), whose simple calculation method has been presented above.

A method for modeling a volume hologram by use of a medium consisting of two separated thin layers has also been suggested. This approach allows one to find experimentally the precise optimal position of the readout beam. Also, the method makes accessible the modeling and direct visualization of the process of diffraction by thick holograms with arbitrary recording parameters. These procedures could be difficult or impossible as a result of the characteristics of commonly used volume recording media (e.g., short lifetimes, low DE, destructive readout, etc.).

References

1. G. Barbastathis, M. Levene, and D. Psaltis, "Shift multiplexing with a spherical reference beam," Appl. Opt. **35**, 2403–2417 (1996).
2. H. C. Kulich, "Reconstructing volume holograms without image field losses," Appl. Opt. **30**, 2850–2857 (1991).
3. G. Barbastathis and D. Psaltis, "Shift multiplexed holographic memory using the two-lambda method," Opt. Lett. **21**, 4432–434 (1996).
4. H. Kogelnik, "Coupled wave theory for thick hologram gratings," Bell. Syst. Tech. J. **48**, 2909–2947 (1969).
5. R. J. Collier, C. B. Burckhardt, and L. H. Lin, *Optical Holography* (Academic, New York, 1971), p. 271.
6. D. T. Smithey, W. C. Babcock, and J. Millerd, "Holographic data storage using thick bacteriorhodopsin recording materials," in *International Symposium on Optical Memory and Optical Data Storage*, Vol. 12 of OSA Technical Digest Series (Optical Society of America, Washington, D.C., 1996), pp. 407–409.

from u_3 intersect one and only one conical region of the hologram allow one to consider the diffraction in such conical regions independently of each other. It means that the diffraction of the beam u_3 within a region determined by β_k will not be changed after the arbitrary changing of the hologram's structure, as well as the shape of the beam u_3 outside the region. In particular, diffraction by hologram H within a region will be equivalent to the diffraction of the plane wave with spatial frequency β_k on a hologram whose grating vector K varies as a function of y in the same manner as that in the given region of hologram H and is independent of x.

Let us now break this new holographic structure into parallel layers $y_{k-1} < y < y_k$. We choose the thickness of each layer to be thin enough to consider $K(y)$ to be constant within the layer. In this case the intensity change of the incident plane wave within each layer can be calculated in accordance with the coupled-wave theory. We can see from Eq. (2.5) below that the equation describing the diffraction depends on only the Bragg mismatch angle δ if we use a first-order Taylor approximation for δ and K. It means that changing the value of K in any layer without changing δ does not change the intensity of the incident beam in the output plane of the hologram. This, in turn, means that the grating vector K can be chosen to have the same value for all layers with the condition that δ is constant. Thus, assuming δ is not changed along the propagation path of the cone of rays constituting u_3, we can calculate the output intensity by calculating the diffraction of the plane wave on the equivalent diffraction grating. The spatial frequency of the plane wave and the absolute value of the grating vector K have to be chosen to be equal to β_k and $K(x, 0)$, respectively.

As indicated in Fig. 1, rays from the recording (x_1, y_1), (x_2, y_2) and reconstructing (x_3, y_3) sources traveling to an arbitrary point $(x, 0)$ on the recording medium make an angle θ_i, where

$$\theta_i(x, y) = \arctan\left(\frac{x_i - x}{y_i - y}\right), \qquad i = 1, 2, 3. \quad (2.1)$$

The Bragg angle at the same point is

$$\theta_{\text{Bragg}}(x, y) = \arcsin\left\{\frac{\lambda_1}{\lambda_2}\sin\left[\frac{\theta_1(x, y) - \theta_2(x, y)}{2}\right]\right\}$$
$$+ \frac{\theta_1(x, y) + \theta_2(x, y)}{2}, \quad (2.2)$$

which follows directly from the Bragg law written in common form[2] for readout λ_2 and recording λ_1 wavelengths. Consequently, the Bragg mismatch angle δ_{Bragg} is

$$\delta_{\text{Bragg}}(x, y) = \theta_{\text{Bragg}}(x, y) - \theta_3(x, y). \quad (2.3)$$

We choose the coordinates of the point-source reconstruction beam (x_3, y_3) in such a way that two of its rays crossing the hologram at points $(0, 0)$ and $(c, 0)$ make Bragg angles with the input plane [Eq.
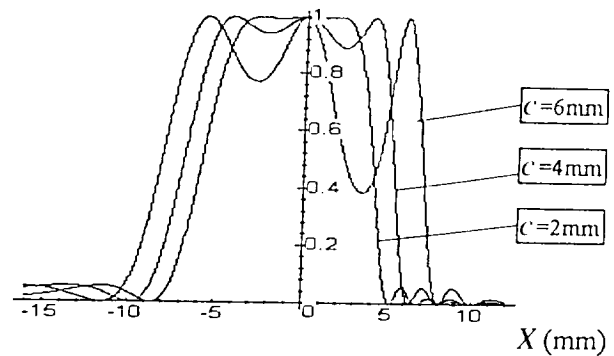
Fig. 2. Normalized DE of $H(0, 0)$ versus the hologram plane position for various values of the parameter c.

(2.2)]. Using geometric construction we can show that

$$y_3 = c\,\frac{\cos[\theta_{\text{Bragg}}(0, 0)]\cos[\theta_{\text{Bragg}}(c, 0)]}{\sin[\theta_{\text{Bragg}}(0, 0)] - \theta_{\text{Bragg}}(c, 0)]},$$

$$x_3 = y_3\,\tan[\theta_{\text{Bragg}}(0, 0)]. \quad (2.4)$$

We then determine the mismatch angle δ_{Bragg} for the rest of the rays of the reconstructed beam and insert it into the relation that expresses the angular sensitivity of a thick hologram:

$$\eta = \left| \exp\left[-\frac{\alpha d}{c_s}\right] \right.$$

$$\left. \times \exp[-i\xi]\,\frac{\exp[i(\xi^2 + \nu^2)^{0.5}] - \exp[-i(\xi^2 + \nu^2)^{0.5}]}{2\left(1 + \frac{\xi^2}{\nu^2}\right)^{0.5}} \right|^2, \quad (2.5)$$

where $\xi = (2\pi n/\lambda_2)\delta_{\text{Bragg}}\,d\,\sin[(\theta_1 - \theta_2)/2]$, with $\nu = \chi d/c_s$, $c_s = \cos[(\theta_1 - \theta_2)/2]$, d is the thickness of the hologram, and χ is the coupling constant.[4]

Expression (2.5) describes, in the exit plane of the hologram, the profile of the intensity of the diffracted wave that attains its maximum at points $x = 0$ and $x = c$. Note that we are interested in the relative DE of diffracted rays versus only δ_{Bragg} for each of them, so we can simplify Eq. (2.5) to obtain

$$\frac{\eta}{\eta_0} = \nu^2\,\text{sinc}^2\{\pi^{-1}[\nu^2 + k\delta_{\text{Bragg}}^2(x, y)]^{0.5}\}. \quad (2.6)$$

Here we took into account the fact that the presence of loss has very little influence on the angular sensitivity[4] and used Eq. (2.5) as written for lossless gratings with real χ. The constant ν was measured experimentally.

Figure 2 represents the relative-intensity distribution profile (equivalent to the normalized DE) of diffracted beams in the exit plane of the hologram calculated for the elemental hologram $H(0, 0)$ (corresponding to the zeroth-order component of the Fou-
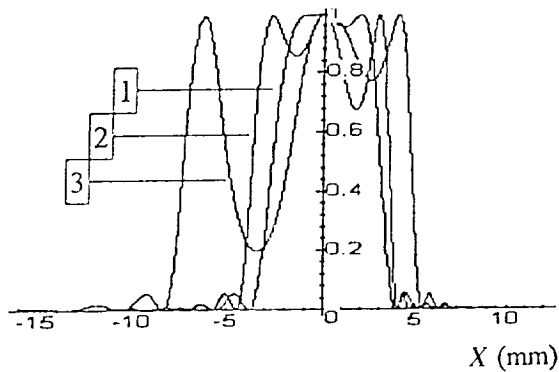
Fig. 3. Normalized DE for cases $(x_1, y_1) = (7, 10)$, $(x_2, y_2) = (6.5, 10)$ (plot 1), (8, 10) (plot 2), (5, 10) (plot 3).

rier spectrum T of transparency t) for reconstructed beams with different values of the parameter c. Values of $\lambda_1 = 458$ nm and $\lambda_2 = 633$ nm were used for this and subsequent plots. The X axis is in the hologram recording plane, and the different values of c are obtained by the changing of the location of the reconstruction point source (x_3, y_3). Optimized readout parameters correspond to the portion of the hologram where the curves of Fig. 2 have sufficient DE, say not less than $1/e$ (as for the definition of the width of a Gaussian-shaped signal), and are as flat as possible. In our experiments (Section 3) the hologram was approximately 3 mm in extent, so $c = 2$ mm would be optimal from Fig. 2.

Profiles of diffracted beams with the optimized parameter c, calculated for several recording setups of $H(0, 0)$ holograms (with different orientations and average spatial frequencies of their recording beams), are shown in Fig. 3. The diffraction of the beam optimized for the reconstruction of hologram $H(0, 0)$ from holograms $H(\Delta x, \Delta y)$, which correspond to the higher-order components of the Fourier spectrum T, is shown in Fig. 4. These plots represent the sum intensity distribution of beams diffracted by elemental holograms $H(\Delta x, \Delta y)$ and $H(-\Delta x, -\Delta y)$, where we use the fact that symmetric components of the Fourier spectrum contain the same information. From Fig. 4 we can see that the relative DE decreases with increasing values of r, corresponding to holograms of higher components of the Fourier spectrum T. Thus the reconstruction system acts like a low-pass filter,
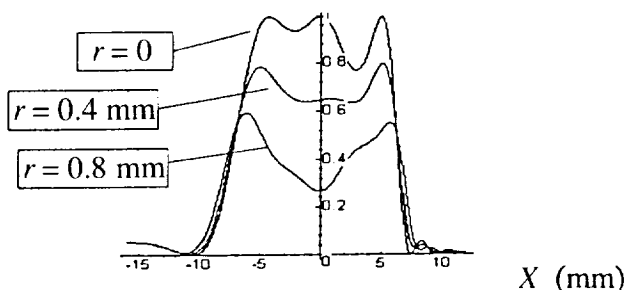
and one can use this curve to define an effective spatial cutoff frequency at some particular value of the relative DE ($1/e$ in this paper).

Let us now consider in more detail how the intensity profiles of beams diffracted by elemental holograms (Figs. 2–4) can be utilized to determine the resolution and intensity distribution in the reconstructed image t. Each point P of the recording transparency t is formed by a cone of rays connecting it with points of the Fourier spectrum (Fig. 1), each of which we took as an elementary point-source object beam of the elemental hologram. The part of the transparency t in the vicinity of the point P will be reconstructed with a resolution h if all rays of a cone with a base radius of
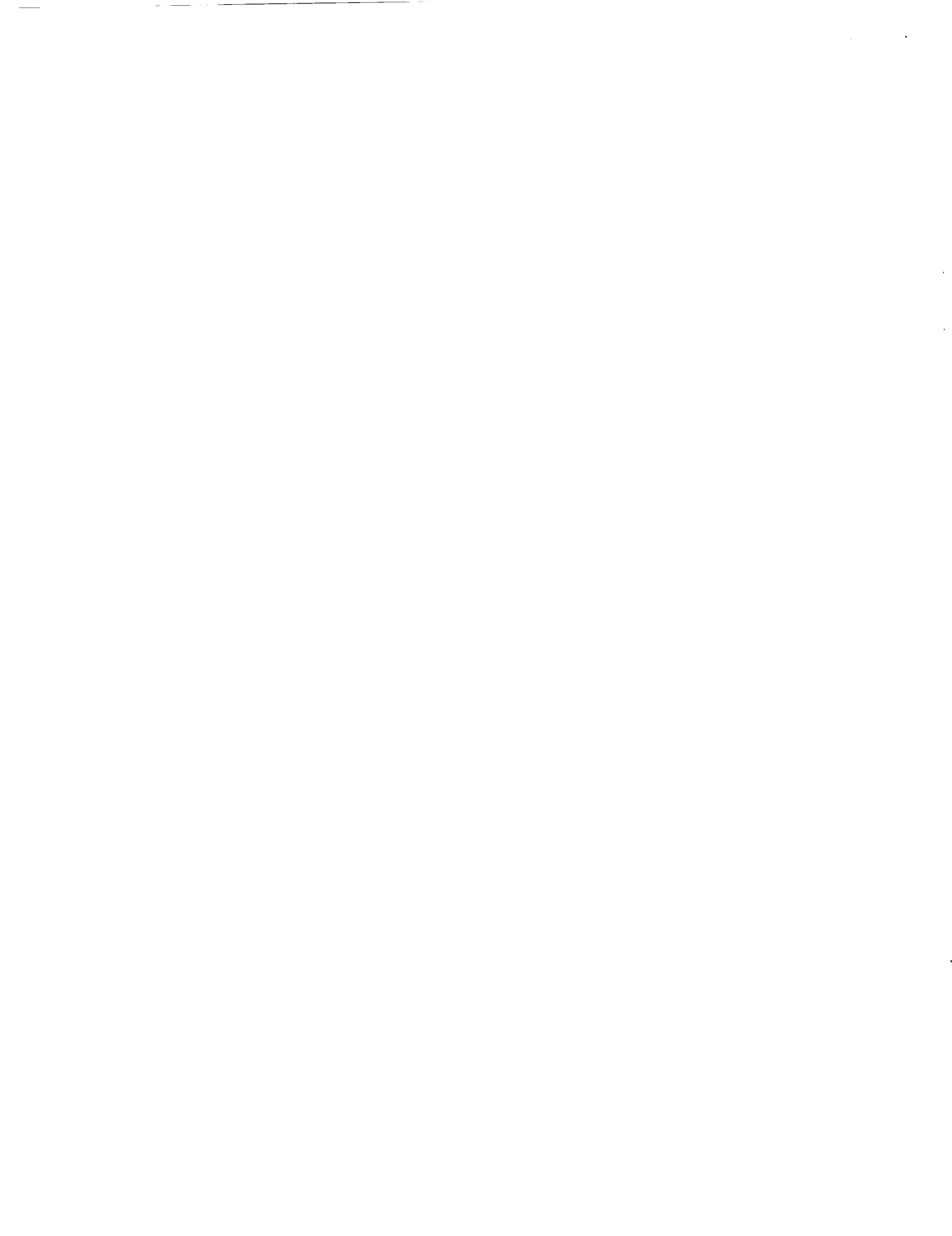
$$r = \frac{0.61\lambda_1 D}{h} \qquad (2.7)$$

have enough DE ($\eta > \eta_0/e$), where $r = (\Delta x^2 + \Delta y^2)^{0.5}$ is one of the coordinates of the Fourier plane of the transparency t and D is the distance between the plane of transparency t and its Fourier transform plane T.[5] If the behavior of the plots in Fig. 4 is taken into account, the proper DE of only edge cone rays corresponding to the maximum-order components of the Fourier spectrum will provide the required resolution. Then it is easy to see that the intensity distribution of the reconstructed beam at the image plane corresponds to a profile of the beam diffracted by the $H(0, 0)$ hologram at its exit plane, reduced in size by $D_2 \cos \theta_{aver}/D_1$, where D_1 and D_2 are the distances between the Fourier plane of image i and, accordingly, the hologram and the plane of the image, respectively, and θ_{aver} is the average incident angle of the reconstructing beam. Thus the intensity and resolution in an arbitrary part of the reconstructed image T can be estimated by the profiles of two beams diffracted by elemental holograms $H(0, 0)$ and $H(\Delta x, \Delta y)$, where Δx and Δy obey the condition of Eq. (2.7).

Let us also consider the limits that the assumptions defined above place on the thickness of the hologram (more exactly, on the Klein parameter Q, which characterizes thick gratings[5] for which the theory is valid). Calculations [Eqs. (2.1)–(2.6)] showed that, for a thickness of approximately 0.5 mm and values of the Q factor of the order of 10^4, the values of δ variations along the propagation path of the reconstructing beam do not exceed 10^{-4} rad, which corresponds to a percent error in the intensity calculation of not more than 5%–7%.

3. Experimental Results

To investigate the different wavelength regimes of recording and reconstructing volume holograms we used a thick BR film. This material exhibits excellent properties for real-time optical processing applications, as well as for permanent high-density data storage.[6] Hologram recording in BR films was carried out in the M-type regime, in which red readout light provided at the same time excitation for the BR

Fig. 4. Normalized DE of elemental holograms with various values of r versus the hologram plane position.

Applications of Bacteriorhodopsin for Optical Data Storage and Processing

Presenter: David J. Mehrl

Optical Systems Laboratory(OSL)

Department of Electrical Engineering (TTU)

Texas Tech University, Lubbock, TX

Colleagues: J. Walkup, T. Krile & A. Bablumian*

*Dr. Arkady Bablumian is a Research Associate currently with the OSL group, and is conducting the bulk of this research.

11/7/97

Foils — Invited

presented ...

What is Bacteriorhodopsin(BR)?

- A polycrystalline protein extracted form a naturally occurring salt marsh bacterium *Halobacterium Halobium*(purple membrane). Used to allow the bacteria(as a "backup" mechanism) to survive by photo-synthesizing energy from the sun, when, e.g.. competing algae deplete the water of oxygen.

Features of BR

- Very robust to extreme environments(e.g. temperature extremes) due to its polycrystalline nature. Relatively inexpensive to process into high quality optical films that can be deposited on planar or even convex surfaces.

- Spatial resolution limited by molecular size (~5 nm) and diffusion (diffusion problems are currently being addressed).

- High sensitivity(1-80 mJ/cm^2), relatively high diffraction efficiency (1-7% typical), fast response (<50μs), excellent stability.

- "Bi-stable" photochromic response.

- Comes in native and mutant* forms (D96N). Also "purple membrane" and more recently "blue membrane" forms.

  * – (whereas native BR are grown in salt water, mutant forms are grown in Lubbock City tap water).

BR as a Spatial Light Modulator

- By performing simultaneous readout (with red light) and writing (with blue-green light), BR can act as a real-time SLM "spatial light modulator". By also using holographic techiques, diffraction efficiency can also be improved. (>5% now).

- A pair of strong write beams(blue) write a grating into the BR material. This grating diffracts the read beam (red). A white light source is then used to project an image onto the BR film, selectively "eroding" parts of the grating. Thus the read beam now carries the(negative) image.

- Can be used, e.g., to convert from incoherent to coherent light, similar to more expensive LCLV SLMs.

BR as a memory - problems

- BR memory retention times are limited (typically hours to days).

- Destructive readout problem reduces BR to "write often/ but read only occasionally" access, unless a judicious refresh scheme is employed.

- **Reading out a page partially erases all pages within the volume.**

- Could be remedied by development of electrical fixing techniques, which are currently being investigated, e.g., by Bend Research, Inc..

BR as a memory-problems

- The touted spatial resolution of >1000 lines/mm is in practice often reduced greatly due to diffusion. Diffusion also severely degrades memory retention times in holographic applications. A recent development (by Bend Research) promises to largely remedy this problem.

BR as a memory - problems

- The "destructive write" problem indirectly causes the achievable diffraction efficiency to decrease geometrically with the number of pages simultaneously stored in the same volume.

- **Writing a page to memory partially erases all previously written pages.**

- This problem cannot be remedied by "fixing" techniques, but can be partially addressed by "exposure scheduling" techniques.

Motivation for Multiplexing
Pages of Data

- Natural for many "data objects" to be stored/retrieved in page format. E.g. images, audio samples, data files etc.. Page access allows "parallel" access to the object data, instead of the usual serial bitstream access normally used in conventional memories.

- High density optical disks-employ simple spatial multiplexing & use thin films. Multiple data objects cannot be stored "on top of each other". **Holographic multiplexing** allow use of "thick" optical films, and multiple pages of data can be stored, and later retrieved from within the same volume. The additional storage volume afforded by increasing the film thickness allows the information per unit surface area (bits/mm^2)to be increased dramatically. (Current research with photorefractives such as Lithium Niobate --> 100's of pages).

Volume Multiplexing Techniques, what's behind them?

<u>Angle multiplexing</u>: Optical signal beam (carrying page of data) is mixed with a carrier beam (the reference beam). Resulting (spatially) heterodyned signal is then recorded as an intensity interference pattern in the BR medium.

Can later retrieve a particular data page by illuminating BR with the original carrier (reference beam).

Angle multiplexing is analgous to "frequency division multiplexing". Direct analogy between the spatial angle $\Delta\theta$ between interfering beams and the "spatial frequency" (ρ - lines/mm) of the "grating-like" intensity interference pattern that is written into the BR medium. [$\rho = (2/\lambda)\sin(\Delta\theta/2)$].

$\rho = \Delta\theta/\lambda$ (lines per mm) -   for small $\Delta\theta$

Simplest reference beam used in angle multiplexing:

Plane wave: $(E_{ref})_i = E_o \cos[k(x \cdot \sin\theta_i + z \cdot \cos\theta_i)]$ $(k=2\pi/\lambda)$

Here E is a time-independent phasor representation that describes the spatial distribution of the field of the light (in this case, the reference light beam). Generally complex-valued where $|E|^2$ describes the intensity of the light, and Arg(E) describes the shapes of the wavefronts.

Orthogonal "Carriers"

Necessary properties for a family of "carriers" used in volume multiplexing - should form an orthogonal basis, i.e. the projection of "basis vectors" onto each other in "Hilbert space" should approach zero. Examples include:

- Family of Plane waves travelling at different angles.
- Family of Plane waves with different wavelengths (WDM)
- Family of Spherical waves "converging to" or "diverging from" noncoincidental point sources.
- Waves using "random phase encoding" of wavefronts.
- Combinations of the above.

Systems Level View of Holographic Recording and Reconstruction

The intensity interference pattern stored in the (BR) medium:

$$I_{rec} = |E_{ref} + E_{sig}|^2 = |E_{sig}|^2 + |E_{ref}|^2 + E^*_{ref} E_{sig} + E_{ref} E^*_{sig}.$$

- The reconstructed signal is proportional to:

$$E_{ref}I_{rec} = E_{ref}|E_{sig}|^2 + E_{ref}|E_{ref}|^2 + E_{ref}E^*_{ref} E_{sig} + E_{ref}E_{ref} E^*_{sig}.$$

- The **third term** contains the original recorded signal data:

$$E_{ref}E^*_{ref} E_{sig} = |E_{ref}|^2 E_{sig} = I_{ref} E_{sig}. \quad (I_{ref} \text{ is usually relatively constant}).$$
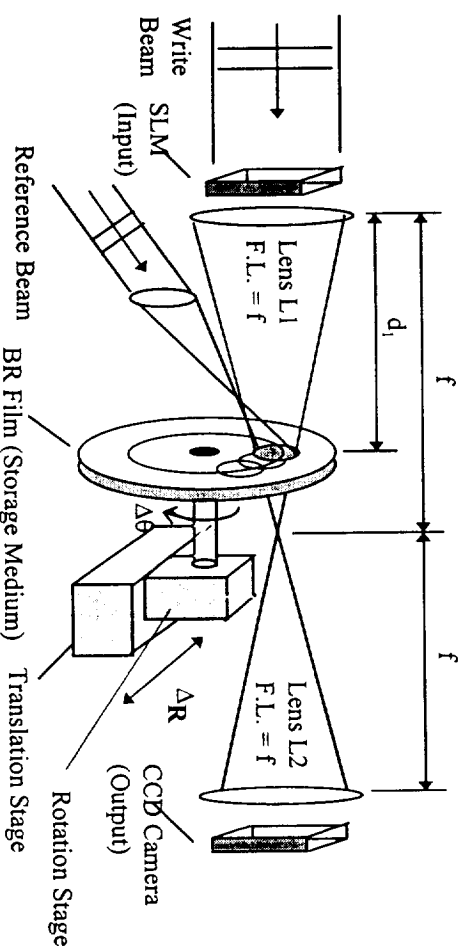
Shift Multiplexing

- In shift multiplexing, the "carriers" can be though of as wideband "chirped" FM carriers reminiscent of techniques sometimes employed in "spread spectrum" communications. Usually the reference beam is a plane wave, but the "signal" beam is a spherical wave, and the interference pattern takes the form of a chirp (with a spatially varyiant instantaneous spatial frequency).

- In our technique, both reference and signal beams are spherical waves.

Shift multiplexing: Relatively simple to implement, and compatible with current optical and magnetic disk read/write access mechanisms.

## Setup for "Shift" Multiplexing of Holographic Data Pages

Write Beam

SLM (Input)

Lens L1 F.L. = f

d_1

f

f

Lens L2 F.L. = f

CCD Camera (Output)

Reference Beam

BR Film (Storage Medium)

$\Delta\theta$

ΔR

Translation Stage

Rotation Stage

Shift translation:

- "Carrier" takes the form of a "spherical wave". After a page of data is recorded, the BR medium is shifted (translated) slightly by mechanical actuators:

- Instead of recording a direct image of data page, a lens is used to perform a "Fresnel transform" of the data. Data associated with each data bit is stored in a "distributed" manner throughout the BR volume.

- Upon readout, a second lens can be used to reconstruct the original image of the data page.
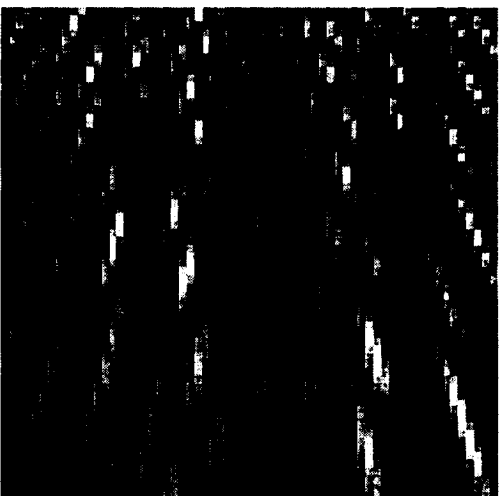
(a.)
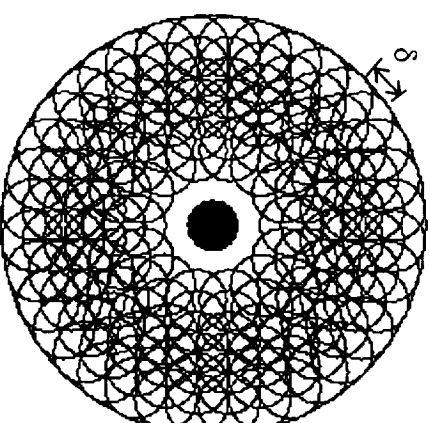
(b.)

Figure 3: (a.) Depiction of three superimposed gratings in a local volume.
(b.) Depiction of page addressing in shift multiplexing, where each circle denotes a page of stored data.

Note multiple data pages are stored within a common volume, by virtue of the "overlapping" of pages (circular regions).

2-λ multiplexing

- It is desirable to write to BR at one wavelength(λ_1), and read it out at another (λ_2). For example, let λ_1 correspond to the 570nm absorptance peak for good write sensitivity, and read it out at λ_2=500nm where there is a large refractive index modulation, but absorptance is reduced. In this way the "destructive readout" problem can be reduced considerably.

- The index of refraction modulation tends to be greatest at wavelengths where the absorptance changes most rapidly with wavelength (i.e. where $|d\alpha(\lambda)/d\lambda|$ is maximal).

- Use of differing wavelengths introduces unique problems when employing holographic volume multiplexing.

Setup for 2-λ Shift Multiplexing in BR
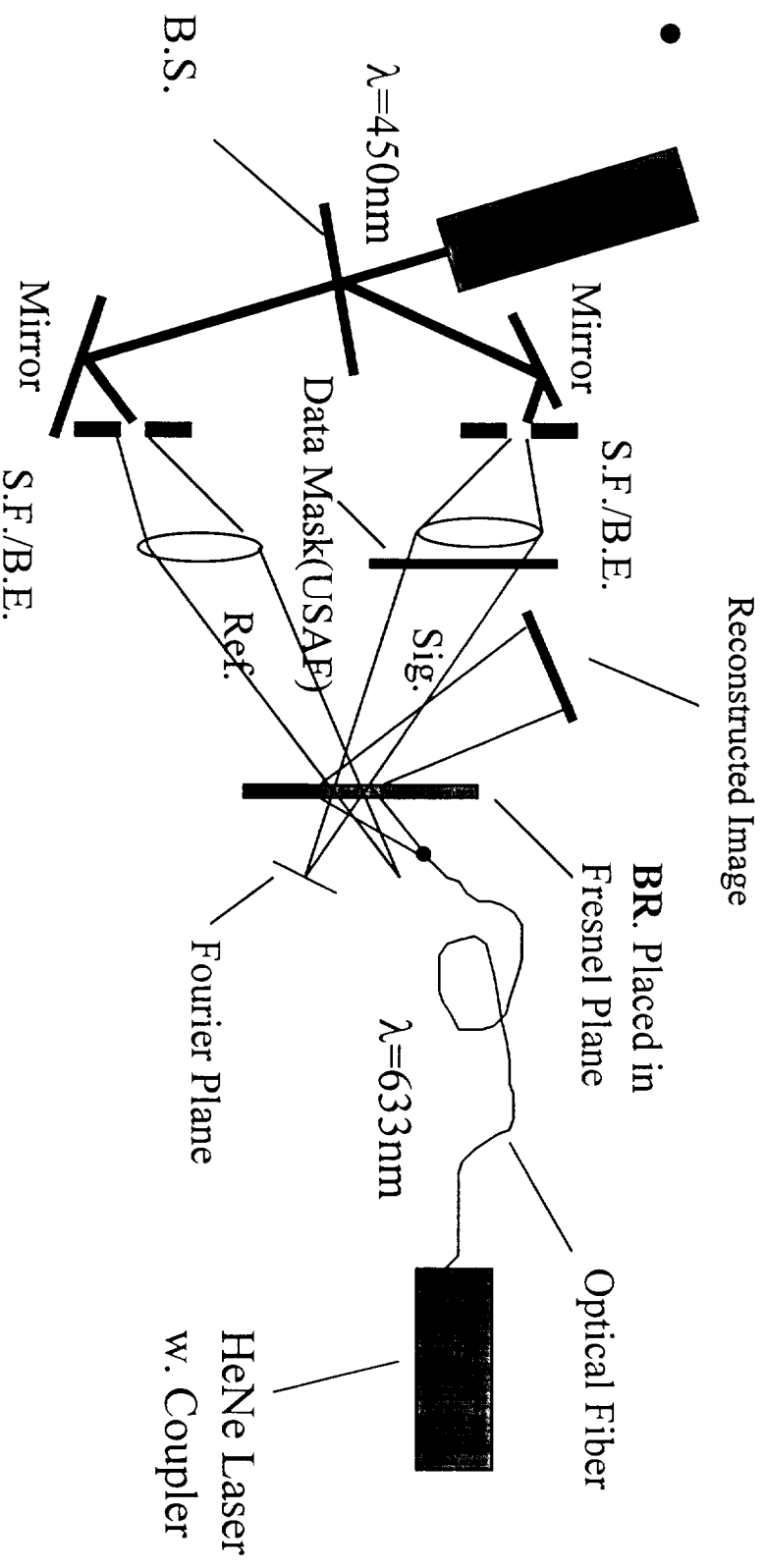
- Phase conjugate reconstruction source @ 633 nm. Some (spatially variant) Bragg mismatch is inevitable over regions of the active recording area.

Issues associated with this approach

- A space-variant Bragg mismatch effect limits the spatial resolution of the reconstructed image (but not too badly).

- The reconstructed image is relocated in space, and (in our case) reduced in size. This effect, however, is inconsequential.

- Use of "point sources" allows use of optical fibers
  - (hence system is compact, and easier to align).

Alignment Issues

- The tip of the "readout fiber" must be aligned to tolerances of a few microns in 3-D space. Dr. Arkady Bablumian has developed a clever experimental technique to facilitate alignment.

- High sensitivity to alignment actually indicates that the system is doing its job! As we use spatial read/write access techniques (e.g. as opposed to WDM), spatial alignment sensitivity comes with the territory if we are to multiplex many pages of data.

Concluding Remarks

- BR has many critical issues that need to be addressed before BR memory becomes practical. Yet many of these issues are also faced by "competing" optical materials such as photorefractive materials and photopolymers.

- One of the most attractive applications we have found for BR is in real-time signal/image processing applications (using BR as a holographic spatial light modulator), but this is not what we are being funded to research.

- The read/write access technologies developed in our research are portable to many other optical materials as well.